TITLE:

Uncertainty assessment of water resources and long-term hydropower generation using a large ensemble of future climate projections for the Nam Ngum River in the Mekong Basin

AUTHOR(S):

Meema, Thatkiat; Tachikawa, Yasuto; Ichikawa, Yutaka; Yorozu, Kazuaki

CITATION:

Meema, Thatkiat ...[et al]. Uncertainty assessment of water resources and long-term hydropower generation using a large ensemble of future climate projections for the Nam Ngum River in the Mekong Basin. Journal of Hydrology: Regional Studies 2021, 36: 100856.

ISSUE DATE:

2021-08

URL:

http://hdl.handle.net/2433/276937

RIGHT:

© 2021 The Authors. Published by Elsevier B.V.; This is an open access article under the CC BY-NC-ND license.

京都大学学術情報リポジトリ
KURENAI
Kyoto University Research Information Repository

京都大学 KYOTO UNIVERSITY
A Self-archived copy in
Kyoto University Research Information Repository
https://repository.kulib.kyoto-u.ac.jp
京都大学学術情報リポジトリ KURENAI 紅 Kyoto University Research Information Repository

Journal of Hydrology: Regional Studies 36 (2021) 100856

Contents lists available at ScienceDirect

Journal of Hydrology: Regional Studies

journal homepage: www.elsevier.com/locate/ejrh

Uncertainty assessment of water resources and long-term hydropower generation using a large ensemble of future climate projections for the Nam Ngum River in the Mekong Basin

Thatkiat Meema *, Yasuto Tachikawa, Yutaka Ichikawa, Kazuaki Yorozu

Department of Civil and Earth Resources Engineering, Kyoto University, Kyoto, Japan

ARTICLE INFO

Keywords:
Climate change
Hydropower
Uncertainty assessment
Distributed hydrologic model
Streamflow projection

ABSTRACT

Study region: The Nam Ngum River Basin, the major tributary of the Mekong River, is located in the Laos PDR.
Study focus: This study aims to assess the sensitivity of Nam Ngum 1 reservoir operation to water resource uncertainty driven by a combination of climate change and upstream cascade dam development.
New hydrological insights for the region: Precipitation projections of the basin under a 4° increase scenario vary in the range of −9.6 % to +6.9 %, compared to the historical observed precipitation (present climate). The impact of climate change on hydropower resources was investigated. Based on the combined effect of climate change and upstream cascade dam development, the projected inflow of the Nam Ngum 1 reservoir at the full development stage will change from −16.0 % to +6.5 %, which results in a large range of annual energy production changes from −18.8 % to +2.8 % compared to the current condition (present climate and existing dam stage). Furthermore, water losses from the reservoir due to water discharge from the spillway for extreme floods and evaporation are expected to increase with increasing temperature, which will lead to a loss in energy production. Our study indicates that the operation of hydropower should be adapted to the effects of climate change. This information can be used by stakeholders to propose water resource management strategies.

1. Introduction

The Mekong flows southward for approximately 4,800 km from its source (Tibetan Plateau) through China, Myanmar, Lao PDR, Thailand, and Cambodia before entering the South China Sea via a complex delta system in Viet Nam with an approximately 795,000 km^2 of the total basin area. The Mekong River ranks 10th among the world's great rivers based on mean annual flow (MRC, 2005). Rapid regional growth and energy demands from neighboring countries have prompted the construction of numerous dams along the mainstream and tributaries of the Mekong River (Kummu and Varis, 2007).

The catchment area of Mekong River in Laos PDR is approximately 25 % of the total basin and contributes 35 % of the total flow into the river, which is considered to be the country with the highest contribution in the Mekong River Basin (MRB) (MRC, 2005). The country has benefits in terms of topography and water resources, which provide significant potential for hydropower development.

* Corresponding author at: Department of Civil and Earth Resources Engineering, Kyoto University, C1, Nishikyo-ku, Kyoto, 615-8540, Japan.
E-mail address: meema.thatkiat.42r@st.kyoto-u.ac.jp (T. Meema).

https://doi.org/10.1016/j.ejrh.2021.100856
Received 19 January 2021; Received in revised form 11 June 2021; Accepted 18 June 2021
Available online 24 June 2021
2214-5818/© 2021 The Authors. Published by Elsevier B.V. This is an open access article under the CC BY-NC-ND license (http://creativecommons.org/licenses/by-nc-nd/4.0/).

京都大学 KYOTO UNIVERSITY
A Self-archived copy in
Kyoto University Research Information Repository
https://repository.kulib.kyoto-u.ac.jp
京都大学学術情報リポジトリ KURENAI 紅 Kyoto University Research Information Repository

ADB (2019) reported that the country's exploitable hydro potential is estimated to be 23,000 MW, and 5,172 MW of hydropower capacity had been operated as of 2017. Based on an analysis of projects to be completed by 2030, total hydropower build-out for both domestic and export use will total 16,500 MW or around 70 % of the estimated potential. However, large variations in changes in hydropower generation across regions and even within regions due to the effects of climate change have been reported (Hamududu and Killingtveit, 2012). The uncertainty of future hydropower generation is derived not only by the current river flow inter-annual variation but also by the change in long-term river flow availability due to the effect of climate change (Blackshear et al., 2011).

Several previous studies have assessed the impact of climate change on hydropower generation on a global scale (Hamududu and Killingtveit, 2012; van Vliet et al., 2016), continental-scale (IEA, 2020; Lehner et al., 2005), national scale (Grijsen and Patel, 2014; Fan et al., 2020), and basin-scale (Beyene et al., 2010; Kopytkovskiy et al., 2015; Mohor et al., 2015; Shrestha et al., 2016). Some studies have been conducted on the impact of climate change on hydropower generation in the MRB. The Mekong River Commission (MRC, 2018) reported that the percentage change in the average energy production of hydropower in Laos PDR for the climate change scenarios during 2060 (RCP2.6 − 8.5) compared to the baseline ranges from +7.5 % to −31.1 %. Piman et al. (2015) reported that there was a minor decrease in hydropower energy production in the Mekong tributaries—Srepok, Sesan, and Sekong (3S) basins—during full development driven by A2 and B2 emission scenarios (MPI_ECHAM4) compared to the baseline scenario.

However, the significant uncertainty in hydropower production assessment is associated with the variability of precipitation projections (Hamlet et al., 2010) resulting from the use of different general circulation models (GCMs). The model projections are affected by a range of uncertainties, including emissions scenario uncertainty, internal variability of the climate system, and model response uncertainty (Hawkins and Sutton, 2009). The quantification of all aspects of model uncertainty requires multi-model ensembles, ideally as a complement to the exploration of single-model uncertainties through perturbed physics ensemble experiments (Tebaldi and Knutti, 2007). Several studies have applied a large ensemble to improve the uncertainties of future river discharge projections (Ayers et al., 2016; Mohammed et al., 2015; Thompson et al., 2017). Carvajal et al. (2017) used a large-ensemble (CMIP5) to assess the sensitivity and improve the reliability of hydropower generation to uncertain water resource availability driven by future climate change in Ecuador. The database for policy decision making for future climate change (d4PDF) is a large GCM ensemble database with a high-resolution model that permits the analysis of long-term trends and future changes in localized and severe events (Mizuta et al., 2017). A number of studies have adopted the database to project future hydroclimates, such as precipitation (Endo et al., 2017; Hibino et al., 2018), extreme floods, and river discharge (Tanaka et al., 2020; Hanittinan et al., 2020).

Information about the adaptability of hydropower generation to hydrologic changes and global warming effects in the region is scarce, especially for large-scale dams in the main tributaries of the Mekong. Thus, this study aims to assess the combined impacts of climate change and dam development in a tributary of the Mekong River in Laos PDR (Nam Ngum River) on hydropower generation using a large ensemble of climate projections. For this purpose, a physically based distributed hydrologic model (Meema and Tachikawa, 2020) was adopted with the projected climate variables using the delta method for different climate scenarios obtained from a large GCM ensemble database, d4PDF. The mean of the projected climate ensembles from each climate scenario was used to evaluate the change in water resources and power production at different dam development stages of the basin. Furthermore, the results of the study demonstrate that implementation strategies for an adaptive reservoir operation are needed to mitigate the impact of climate change.

2. Description of study area

2.1. Nam Ngum River Basin

The Nam Ngum River Basin (NNRB) is the main Mekong tributary located in the central part of Lao PDR. The basin is one of the most significant areas in Lao PDR in terms of size (approximately 16,800 km^2 and 7% of the country area). Annual flows contributing to the mainstream of the Mekong River are approximately 14 %, which accounts for approximately 40 % of the country's contribution to the Mekong River flow. The headwaters of the Nam Ngum River are at an elevation of 2,800 m in the northeast of the basin and heads southward for 420 km to its outlet at the Mekong River. Downstream of the Nam Ngum 1 reservoir (NN1), the Nam Ngum River has a gentle slope as it meanders along its course. The Vientiane Plain extends from each bank, covering an area of approximately 2,000 km^2 at elevations of 160–180 m. During the wet season, the plains are influenced by flooding in the floodplain.

The average annual discharge of the Nam Ngum River to Mekong is approximately 21,000 million cubic meters (mcm). The flows are highly seasonal, with low flow occurring from March to April and high flow occurring from August to September. The Nam Ngum Basin is largely tropical, with a distinct wet season from June to October and a dry season for the rest of the year. The highest temperature is in March and April, where average temperatures range from 30 °C to 38 °C, depending on location and altitude. The lowest temperatures occur between November and February, with an average of 15 °C at higher elevations, the Xiengkhuang Plateau. The mean annual rainfall of the basin is approximately 2,000 mm, ranging from 1,450 mm to 3,500 mm across the basin. The highest amount of rainfall occurred near the Vangvieng area and gradually decreased northeastward to the Xiengkhuang vicinity.

2.2. Water resources development

Currently, six hydroelectricity-related schemes are located in the NNRB with a total reservoir storage of approximately 15,200 mcm and a combined electricity generation capacity of 990 MW. The first hydropower station in the basin was the NN1 reservoir, which was developed in 1971 with an installed capacity of 155 MW. The NN1 scheme, the largest among the six hydropower schemes, has a storage capacity of 7,010 mcm. The Nam Song diversion project (NS_DV), operated in 1996, diverts approximately 3650 mcm/year of

京都大学 KYOTO UNIVERSITY
A Self-archived copy in
Kyoto University Research Information Repository
https://repository.kulib.kyoto-u.ac.jp
京都大学学術情報リポジトリ KURENAI 紅 Kyoto University Research Information Repository

water from the Nam Song River into the NN1 reservoir. The other two hydropower stations, Nam Ngum 2 (NN2) and Nam Lik 1/2 reservoirs, began operation in 2011 with installed capacities of 615 MW and 100 MW, respectively. NN2 is the major power station located upstream of the NN1 reservoir with the largest power capacity and second largest storage volume of 6270 mcm (among the dams in the basin). In 2012, the Nam Ngum 5 (NN5) hydropower station began operation with an installed capacity of 120 MW. The dam is located on the tributary of the Nam Ngum River—Nam Ting River. In addition, the Nam Leuk (NL) and the Nam Mang hydropower dams, located outside of the Nam Ngum Basin, began operation in 2000 and 2005, respectively, diverting water from the NL and Nam Mang basins into the NN1 reservoir and the Vientiane Plain, respectively.

The NNBR has significant hydropower potential with high rainfall and large differences in elevation. An additional four dams are at various stages of development, ranging from planning to construction. In the case where all dams are constructed, the total power generation capacity is 1,900 MW, and the total storage volume is 17,200 mcm, which is approximately 80 % of the total annual river discharge of the Nam Ngum River. The locations of the hydropower stations are shown in Fig. 1, and a list of hydropower stations in the basin is summarized in Table 1.

3. Coupled simulation model for hydrological, reservoir, and hydropower generation

The 1 K-DHM is a distributed hydrological model based on a kinematic wave flow approximation that considers surface-subsurface flow. The elevation and flow direction were determined using topographical data provided by HydroSHEDS (Lehner et al., 2006) with

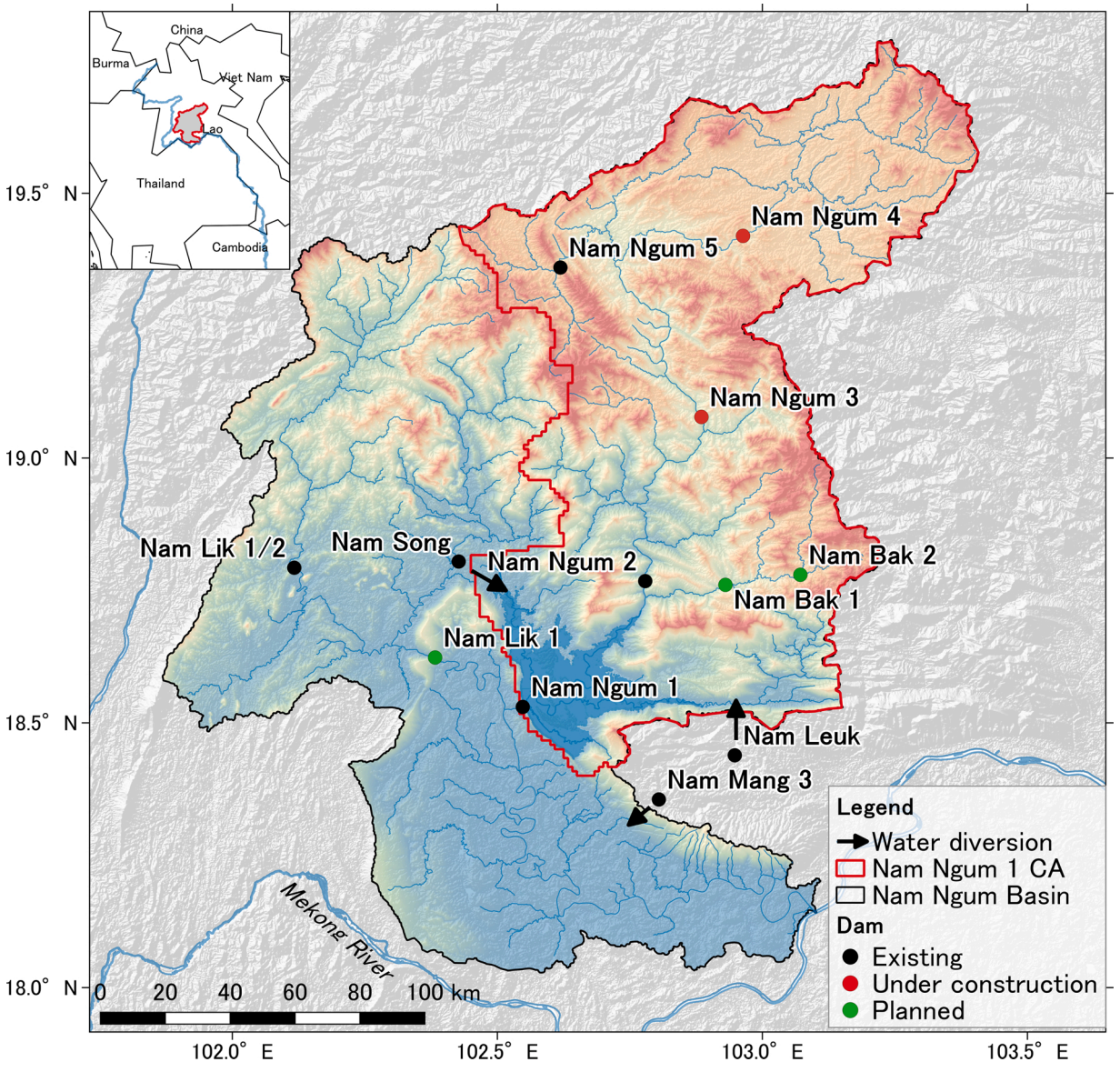

Fig. 1. Location of dams in the Nam Ngum River Basin.

京都大学 KYOTO UNIVERSITY
A Self-archived copy in
Kyoto University Research Information Repository
https://repository.kulib.kyoto-u.ac.jp
京都大学学術情報リポジトリ KURENAI 紅 Kyoto University Research Information Repository

Table 1
List of dams in the Nam Ngum River Basin (E: existing dam, UC: under construction and P: planed dam).

Project	Status	Catchment area (km^2)	Annual inflow (mcm)	Storage at full supply (mcm)	Effective storage (mcm)	Installed capacity (MW)
Within the basin						
Nam Ngum 1	E	8460	12047	7010	4714	155
Nam Ngum 2	E	5640	6270	6774	2617	615
Nam Ngum 3	UC	3888	3090	1407	1070	440
Nam Ngum 4	UC	1748	1512	85.6	72.1	230
Nam Ngum 5	E	483	719	314	72.4	120
Nam Lik 1/2	E	1993	2690	1095	na	100
Nam Lik 1	P	5050	5786	61.3	na	61
Nam Bak 1	P	597	750	250	na	115
Nam Bak 2	P	320	400	190	na	68
Nam Song	E	1303	3072	14.2	na	–
Outside the basin						
Nam Mang 3	E	65	na	45	na	40
Nam Leuk	E	274	438	154	na	60

digital elevation models (DEMs) in 30 s (approximately 1 km) resolution. Meema and Tachikawa (2020) improved the 1 K-DHM for long-term river flow simulation to assess the impact of hydropower operation, and it was extended by incorporating the reservoir-hydropower plant process into the model in the NNRB (Meema et al., 2020). The model was calibrated from 2002 to 2005 in which the hydrologic parameters and reservoir operation of the NN1 (operation rules) were optimized to perform the simulation in agreement with the actual operation record. Validation period 1 (2006–2009) presents the condition without NN2, and validation period 2 (2012–2013) presents the existing condition of the basin (including the NN2). The model showed good agreement between the simulation and reference data (i.e., inflows, regulated discharge, reservoir water level, and energy production) of the NN1 power station during the calibration and validation processes, as shown in the comparison between the simulated result and the record in Fig. 2 and the summary of model performances in Table 2. The calibrated hydrologic parameters and reservoir operation data (rule curve and operation rules) were collected.

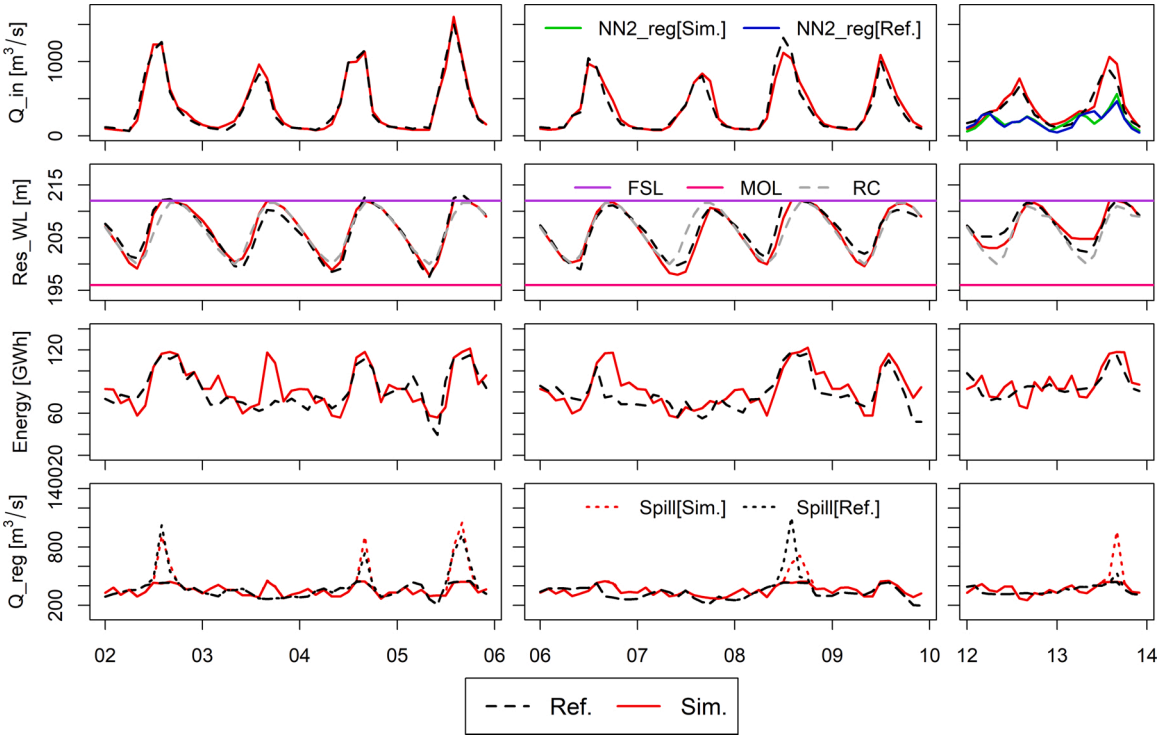

Fig. 2. Comparison of inflow (Q_in), reservoir water level (Res_WL), generated energy (Energy) and regulated flow (Q_reg) between simulation and reference data of the NN1 reservoir (Meema et al., 2020). For the horizontal axis "02 – 06" is calibration period (2002 – 2005), "06 – 10" is validation period 1 (2006 – 2009), and "12 – 14" is validation period 2 (2012 – 2013). (RC: rule curve, FSL: full supply level, MOL: minimum operation level, NN2_reg: regulated discharge by NN2 and Spill: spill discharge through the NN1 spillway).

京都大学 KYOTO UNIVERSITY
A Self-archived copy in
Kyoto University Research Information Repository
https://repository.kulib.kyoto-u.ac.jp
京都大学学術情報リポジトリ KURENAI 紅 Kyoto University Research Information Repository

The coupled 1 K-DHM consists of two main processes, hydrological processes and reservoir-hydropower plant processes, as shown in the schematic drawing in Fig. 3. A general description of each process is discussed in the following subsections.

3.1. Hydrologic processes

Each grid of the hydrological process consists of river and slope flow components (Tanaka and Tachikawa, 2015). To improve long-term river flow simulation, Meema and Tachikawa (2020) improved the structure of the slope flow component by incorporating an unconfined bedrock aquifer layer into the model. A combination of discharge from both layers contributes to the river channel component as the lateral discharge per unit length. The modification of the slope flow model consists of a surface soil layer (original model) and a bedrock aquifer layer. The continuity and momentum equations for the surface soil layer are as follows:

$$\frac{\partial h_s}{\partial t}+\frac{\partial q_s}{\partial x}=r-e-p_u \tag{1}$$

$$q_s(h_s)=\begin{cases} d_m k_m\left(\dfrac{h_s}{d_m}\right)^{\beta} i & (0\le h_s\le d_m)\\ d_m k_m i+(h_s-d_m)k_a i & (d_m\le h_s\le d_a)\\ d_m k_m i+(h_s-d_m)k_a i+\dfrac{\sqrt{i}}{n_s} & (h_s-d_a)^m(d_a\le h_s)\end{cases} \tag{2}$$

where q_s is the runoff per unit slope width, h_s is the water depth, r is the rainfall intensity, e is the actual evapotranspiration, p_u is the vertical infiltration rate from the surface soil layer into the bedrock aquifer, d_m is the maximum water content in the capillary pore, k_m is the hydraulic conductivity when the capillary pore is saturated, β is an exponent parameter that describes the relationship between hydraulic conductivity and water content, d_a is the maximum water content in the effective porosity, k_a is the saturated hydraulic conductivity, n_s is the Manning's roughness coefficient for surface flow, and i is the slope gradient, and $m = 5/3$.

The continuity and momentum equations for bedrock aquifer layer are as follows:

$$\frac{\partial h_u}{\partial t}+\frac{\partial q_u}{\partial x}=p_u \tag{3}$$

$$q_u(h_u)=\alpha_u {h_u}^2 \tag{4}$$

where d_u is the total effective depth of rock fracture in the unconfined bedrock aquifer, h_u is the total water depth in the fracture of the aquifer, $\alpha_u = k_u i/d_u$, k_u is the hydraulic conductivity that corresponds to the actual cross-sectional area of flow in the rock fracture, and i is the gradient of the hillslope.

3.2. Reservoir and hydropower plant processes

Reservoir hydropower plant processes are the processes of reservoir routing and hydropower generation in which the release discharge to the downstream grid is determined using the reservoir guide curve (rule curve) method. Release flows are specified for each time step as well as the reservoir level and spillage. The generated discharge (discharge through the turbines) is determined by using the release decision model based on the multiple zones of the reservoir and their operating rules, as shown in Fig. 4 as an example input to the model for the NN1 reservoir. Fig. 4 includes three curves: the full supply level, guide curve (can have more than one curve for any reservoir), and minimum operation level. The guide curve has two purposes: to guide the reservoir water level (which the model tries as much as possible to follow) and to separate the zones. The zones that are separated are referred to as "the multiple zones of the reservoir." The numbers below the figure (each value for each month in each zone) are the generation time per day in hour, we call this as "operation rules" of the zone. In this study, we collected this value from the actual operation record during the calibration period (2002–2005) as the input of the model. This process provides the target of energy generation that evaluates the release to obtain the reservoir water level to the guide curve (rule curve) at the end of the time step as much as possible based on the starting reservoir water level and current inflow. Reservoir storage is simulated using the laws of mass balance (Meema et al., 2020):

Table 2
Model performances of reservoir simulation for the NN1 power station (Meema et al., 2020). RMSE is the root mean square error in the same unit with the variable and PBIAS is percent bias in %. Q_in is reservoir inflow, Res_WL is reservoir water level, Energy is generated energy and Q_reg is regulated flow.

Variables	Calibration		Validation 1		Validation 2	
	RMSE	PBIAS	RMSE	PBIAS	RMSE	PBIAS
Q_in (m^3/s)	51.9	1.8	82.3	4.9	90.3	8.0
Res_WL (m)	1.0	0.1	1.2	−0.2	1.4	−0.1
Energy (GWh)	13.9	3.5	14.7	6.6	10.3	2.5
Q_reg (m^3/s)	69.2	1.7	99.3	4.3	100.4	8.1

京都大学 KYOTO UNIVERSITY
A Self-archived copy in
Kyoto University Research Information Repository
https://repository.kulib.kyoto-u.ac.jp
京都大学学術情報リポジトリ KURENAI 紅 Kyoto University Research Information Repository

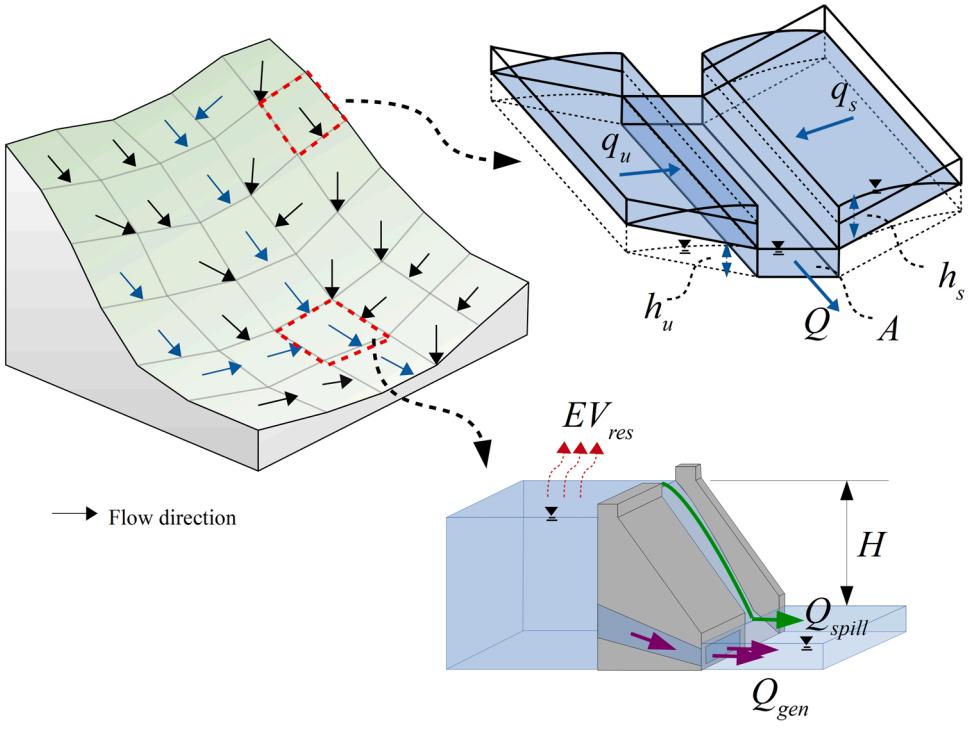

Fig. 3. Schematic drawing of the coupling model.

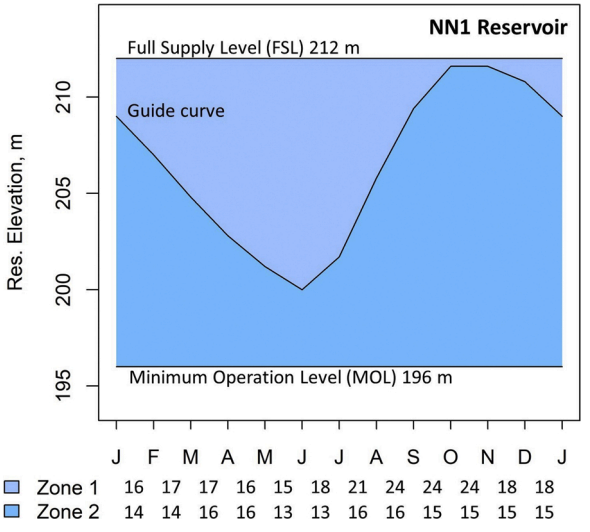

Fig. 4. The multiple zones of the reservoir and their operating rules for the NN1 reservoir (reservoir model input in this study).

$$\frac{dS}{dt} = Q_{in} - (Q_{gen} + Q_{spill}) - Losses \tag{5}$$

where S is the reservoir storage, t is the time, *Losses* is the reservoir loss due to the water surface evaporation estimated using the current reservoir surface area (it is a function of the reservoir water level) and the evaporation rate, Q_{in} is the reservoir inflow, Q_{spill} is the spilled discharge, and Q_{gen} is the generated discharge through the turbine expressed as follows:

$$Q_{gen} = \frac{E}{\eta \cdot \rho \cdot g \cdot H} \tag{6}$$

京都大学 KYOTO UNIVERSITY
A Self-archived copy in
Kyoto University Research Information Repository
https://repository.kulib.kyoto-u.ac.jp
京都大学学術情報リポジトリ KURENAI 紅 Kyoto University Research Information Repository

where E is the generated energy in the time step, η is the turbine efficiency, ρ is the water density, g is the gravitational acceleration, and H is the hydraulic head.

3.3. Estimation of water diversion

To calculate the amount of water diversion, we assigned the amount of water diversion as the boundary condition in the model. The diversion records from 2002 to 2009 for the Nam Song Diversion Dam (NS_DV) and the NL Dam were used to determine the diversion amount from the dams in the present climate scenario.

To predict the amount of water diversion in different climate scenarios, we assumed that the operation of the diversion dams was based on the amount of inflow.

Therefore, we adopted the monthly ratio between the simulated flow in the present climate condition and the discharge of the diversion record; then, we applied the ratio with the simulated river discharge for each climate scenario. The diverted water discharge was limited to the maximum diversion capacity (200 m^3/s for NS_DV and 60 m^3/s for NL). The amount of water diversion can be calculated as follows:

$$Q_{dv\,sim}(i,j) = k(i,j) \cdot Q_{in\,sim}(i,j) \tag{7}$$

where j is month, i is the year (2002, 2003, …, 2009), $Q_{in\,sim}$ is simulated inflow to the diversion dam, $Q_{dv\,sim}$ is simulated diversion discharge, and k is the diversion ratio, which was determined using the following equation:

$$k(i,j) = \frac{Q_{dv_{rec}}^{PS}(i,j)}{Q_{in_{sim}}^{PS}(i,j)} \tag{8}$$

where $Q_{dv_{rec}}^{PS}$ is the record of mean monthly diversion discharge in the present condition and $Q_{in_{sim}}^{PS}$ is the simulation of mean monthly inflow in the present condition.

4. Future climate and simulation scenarios

4.1. Future climate projection data base (d4PDF)

A d4PDF contains the outputs from global warming simulations under the present, 4° (+4 K), and 2° (+2 K) temperature increase conditions using a 60-km atmospheric general circulation model (AGCM). The duration of each experiment was 60 years. Each set of experiments had 100 and 90 ensemble members for the historical and 4° increase experiments in which the initial conditions and the lower boundary conditions were perturbed (Mizuta et al., 2017). The experimental settings are listed in Table 3.

The historical climate was simulated using a 100-member ensemble. The observed monthly mean sea surface temperature (SST), sea ice concentration (SIC) (Hirahara et al., 2014), and climatological monthly sea ice thickness (SIT) (Bourke and Garrett, 1987) were used as the lower boundary conditions of the AGCM.

For the +4 K simulation, the global mean surface air temperature was considered 4 °C warmer than in the pre-industrial era. The greenhouse gases (GHGs) were set to the values in 2090 of the RCP8.5. The climatological SST warming patterns (ΔSSTs) from six CMIP5 models−CCSM4 (CC), GFDL CM3 (GF), HadGEM2-AO (HA), MIROC5 (MI), MPI-ESM-MR (MP), and MRI-CGCM3 (MR)−were added to the observational SST after removing the long-term trend component. The 6 ΔSSTs contained a 15-member ensemble, yielding a total of 90 members.

For the +2 K simulation, the global mean surface air temperature was considered to be 2 °C warmer than in the pre-industrial era and the GHGs were set to the values in 2040 of the RCP8.5 scenario (Fujita et al., 2019). The same six CMIP5 models as in the +4 K simulation were used as the ΔSSTs of the AGCM. Each of the six ΔSSTs contained a 9-member ensemble, yielding a total of 54 members.

Table 3
Simulation settings and description of the period, number of ensembles and future SST change obtained from CMIP5 model.

	Historical simulation	+2 K Future simulation	+4 K Future simulation	CMIP5 model for obtaining ΔSST	
Duration	60 (1951−2010)	60 (2031−2090)	60 (2051−2110)	**Model**	**Institution (Country)**
Members (GCM)	100 (m001-m100)	9 (m101-m109) × 6 SSTs	15 (m101-m109) × 6 SSTs	CCSM4 (CC)	NCAR (United States)
				GFDL CM3 (GF)	NOAA GFDL (United States)
				HadGEM2-AO (HA)	Met Office Hadley Center (United Kingdom)
				MIROC5 (MI)	AORI, NIES, JAMSTEC (Japan)
				MPI-ESM-MR (MP)	Max Planck Institute for Meteorology (Germany)
				MRI-CGCM3 (MR)	Meteorological Research Institute (Japan)
Greenhouse gases	Observed	Values at 2040 of RCP8.5	Values at 2090 of RCP8.5		

京都大学 KYOTO UNIVERSITY
A Self-archived copy in
Kyoto University Research Information Repository
https://repository.kulib.kyoto-u.ac.jp
京都大学学術情報リポジトリ KURENAI 紅 Kyoto University Research Information Repository

4.2. Climate projection scenarios using the delta method

One of the simplest ways to statistically downscale GCM projections is to use the delta or change factor method (Trzaska and Schnarr, 2014). The change factor (Δ) is the ratio between the GCM simulations of future and current climate and is used as a multiplicative factor to obtain future regional conditions. This method assumes that GCMs simulate relative changes more reliably than absolute values (Hay et al., 2000). Therefore, climate variables can be projected as follows:

$$V_F = \Delta(j) \cdot V_{PS} \tag{9}$$

where V_F is the daily mean projected climate variable, V_{PS} is the daily mean present climate variable (observed or reference data), and $\Delta(j)$ is the monthly change factor, which can be calculated as follows:

$$\Delta(j) = \frac{\overline{V}_F^{GCM}(j)}{\overline{V}_H^{GCM}(j)} \tag{10}$$

where j is month and $\overline{V}_H^{GCM}$ and $\overline{V}_F^{GCM}$ are mean monthly values of the GCM variable for historical and future conditions, respectively, which can be calculated as follows:

$$\overline{V}^{GCM}(j) = \frac{\sum_{n=1}^{N} \overline{V}_n^{GCM}(j)}{N} \tag{11}$$

where N is the number of ensembles, j is month, n is the ensemble number (1, 2, 3, …, N), and $\overline{V}_n^{GCM}(j)$ is the mean monthly value of the GCM variable for the ensemble member n, which is calculated as follows:

$$\overline{V}_n^{GCM}(j) = \frac{\sum_{i=1}^{60} V_{n,i}^{GCM}(j)}{60} \tag{12}$$

where j is month, i is the year number (1, 2, 3, …, 60), and $V_{n,i}^{GCM}(j)$ is the monthly value of the GCM variable for the n-th member.

4.2.1. Projection of precipitation

The observed daily rainfall from 2002 to 2009 over the basin was collected to represent the present climate conditions. The future precipitation amounts for different climate scenarios were projected using Eq. (9). To obtain the delta factor of precipitation for each month, monthly precipitation extracted from d4PDF is used as the j-th monthly value of the GCM climate variable ($V_{n,i}^{GCM}(j)$) for the i-th year in the n-th member in Eq. (12). The delta factor of precipitation for different climate scenarios can then be obtained using Eqs. (11) and (10), respectively:

4.2.2. Projection of actual evapotranspiration

To simulate long-term river flow, actual evapotranspiration (AET) is another necessary input parameter; however, it is the most difficult parameter to measure in the field of basin hydrology. Meema et al. (2020) estimated the AET for the NNRB with a daily average of 2.78 mm/day using the water balance method (the difference in the amount of water between annual precipitation and river discharge). For this study, we adopted this information as the AET for the present climate scenario.

To project the future AET in different climate scenarios, Eq. (9) is adopted. To calculate the delta factor for AET, a combination of the simulated amount of water transferred from the global surface into the atmosphere, including the water transpiration from soil (TS), the evaporation on soil (ES), and the evaporation on the leaf (EL) in different climate scenarios obtained from d4PDF, was used as the monthly value of the GCM climate variable in Eq. (12). Then, the delta factor of the AET for different climate scenarios could be obtained using Eqs. (11) and (10), respectively.

4.2.3. Projection of reservoir evaporation

The estimated evaporation from a water body for NNBR with a mean daily value of 2.4 mm/day, estimated by Meema et al. (2020), was adopted as the present reservoir evaporation loss.

For the future projection of reservoir evaporation loss due to climate change (assuming that the pan coefficient of 0.7, has no significant change in future conditions), the delta factor of the basin potential evaporation between historical and future conditions is used to multiply with the present reservoir evaporation, similar to Eq. (9).

To calculate the delta factor of reservoir evaporation, the basin-average mean monthly temperature in different climate scenarios was extracted from d4PDF to estimate the potential evaporation of the basin using the Thornthwaite method (Thornthwaite, 1948), which is used as the monthly value of the GCM variable in Eq. (12). The delta factor can then be calculated using Eqs. (11) and (10), respectively.

4.3. Simulation scenarios dam development and climate change

The combination scenarios between upstream dam development and climate change were conducted to investigate the uncertainty in basin hydrology and dam operation. A list of simulated scenarios is provided in Table 4.

京都大学 KYOTO UNIVERSITY
A Self-archived copy in
Kyoto University Research Information Repository
https://repository.kulib.kyoto-u.ac.jp
京都大学学術情報リポジトリ KURENAI 紅 Kyoto University Research Information Repository

To assess uncertainty due to dam development, three stages of dam development—no dam (ND), existing dam (ED), and future dam (FD)—were conducted. In this study, we focused on a large-scale dam that has many effects on river flow due to its regulation. Based on the large-scale dam criteria in the Mekong tributaries (Piman et al., 2016), NN1 and NN2 met the criteria for the ED stage, whereas Nam Ngum 3 (NN3) met the criteria for the FD stage.

To assess the uncertainty of different climate projections on precipitation and actual evapotranspiration, 15 climate scenarios were established (1 for present, 7 for +2 K, and 7 for +4 K). The present climate scenario (BL) refers to historical data—precipitation and actual evapotranspiration—in the period 2002–2009. The +2 K scenarios used GHG levels at 2040 from RCP8.5 and six warming patterns (ΔSST): +2 K with CC pattern (2K_CC), +2 K with GF pattern (2K_GF), +2 K with HA pattern (2K_HA), +2 K with MI pattern (2K_MI), +2 K with MP pattern (2K_MP) and +2 K with MR pattern (2K_MR)—and +2 K with the mean value of warming patterns (2K_AVR). The +4 K scenario used GHG levels at 2090 from the RCP8.5 and six warming patterns (ΔSST): +4 K with CC pattern (4K_CC), +4 K with GF pattern (4K_GF), +4 K with HA pattern (4K_HA), +4 K with MI pattern (4K_MI), +4 K with MP pattern (4K_MP) and +4 K with MR pattern (4K_MR)— and +4 K with the mean value of warming patterns (4K_AVR).

5. Results and discussion

5.1. Climate change projections

5.1.1. Precipitation

Fig. 5**a** shows the differences between the reference data and the 100-member ensemble d4PDF basin-averaged monthly precipitation estimates. The purpose of this study was to demonstrate the performance of the GCM (d4PDF) in comparison with the observation data. The analysis presented a difference in magnitude with the GCM (d4PDF) over-predicting precipitation during the dry season, especially in March and April, and under-prediction during the wet season in June and July. Conversely, the climate model effectively captured the seasonal variation with the observed data. This demonstrates that the historical experiment of GCM (d4PDF) shows an agreement in seasonal variation with the reference observed data and is appropriate to adopt to project the climate variables from the present climate in various scenarios using the delta change method to assess the uncertainty of climate projections for the NNRB.

Fig. 5**b** illustrates the mean monthly basin precipitation trends for all climate scenarios in the 2° and 4° increase experiments from the GCM prediction. The monthly delta changes factor obtained by analyzing the GCM data set ranged from 0.73 to 1.36 for +2 K scenarios and ranged from 0.71 to 1.50 for +4 K scenarios. This shows that the range of change in precipitation is much larger when the temperature increases. Although the range of the delta change in the dry season seems similar to that in the wet season (0.71 − 1.44 for the dry season and 0.73 − 1.50 for the wet season), a primary difference in the prediction of precipitation magnitude occurs during the wet season, especially in July and August.

By using the delta factors obtained by analyzing the d4PDF dataset with the observed precipitation (present climate), precipitation projections in different climate scenarios were predicted, as shown in Fig. 5**c**. Based on the average daily accumulation for all climate scenarios, the climate projections describe a range of changes in mean annual precipitation (compared to historical observed data) from −5.5 % to +4.9 % for +2 K scenarios and from −9.6 % to +6.9 % for +4 K scenarios. Similar to the delta change factors, a significant change in the amount of projected precipitation occurs in the wet season, especially in July and August.

The average pattern of the +2 K climate scenario (2K_AVR) results in a slight increase (0.35 % increase) in mean annual precipitation compared to the observation (present climate), and a slight reduction (0.64 % reduction) resulted in an average pattern of the +4 K climate scenario (4K_AVR).

Table 4
List of Simulation scenarios.

Climate scenarios	ΔSST	Scenarios		
		Without dam (ND)	Existing dams (ED)	Future dams (FD)
Present	–	ND_PS	ED_PS	FD_PS
+2 K Future	CC	ND_2K_CC	ED_2K_CC	FD_2K_CC
	GF	ND_2K_GF	ED_2K_GF	FD_2K_GF
	HA	ND_2K_HA	ED_2K_HA	FD_2K_HA
	MI	ND_2K_MI	ED_2K_MI	FD_2K_MI
	MP	ND_2K_MP	ED_2K_MP	FD_2K_MP
	MR	ND_2K_MR	ED_2K_MR	FD_2K_MR
	AVR	ND_2K_AVR	ED_2K_AVR	FD_2K_AVR
+4 K Future	CC	ND_4K_CC	ED_4K_CC	FD_4K_CC
	GF	ND_4K_GF	ED_4K_GF	FD_4K_GF
	HA	ND_4K_HA	ED_4K_HA	FD_4K_HA
	MI	ND_4K_MI	ED_4K_MI	FD_4K_MI
	MP	ND_4K_MP	ED_4K_MP	FD_4K_MP
	MR	ND_4K_MR	ED_4K_MR	FD_4K_MR
	AVR	ND_4K_AVR	ED_4K_AVR	FD_4K_AVR

京都大学 KYOTO UNIVERSITY
A Self-archived copy in
Kyoto University Research Information Repository
https://repository.kulib.kyoto-u.ac.jp
京都大学学術情報リポジトリ KURENAI 紅 Kyoto University Research Information Repository

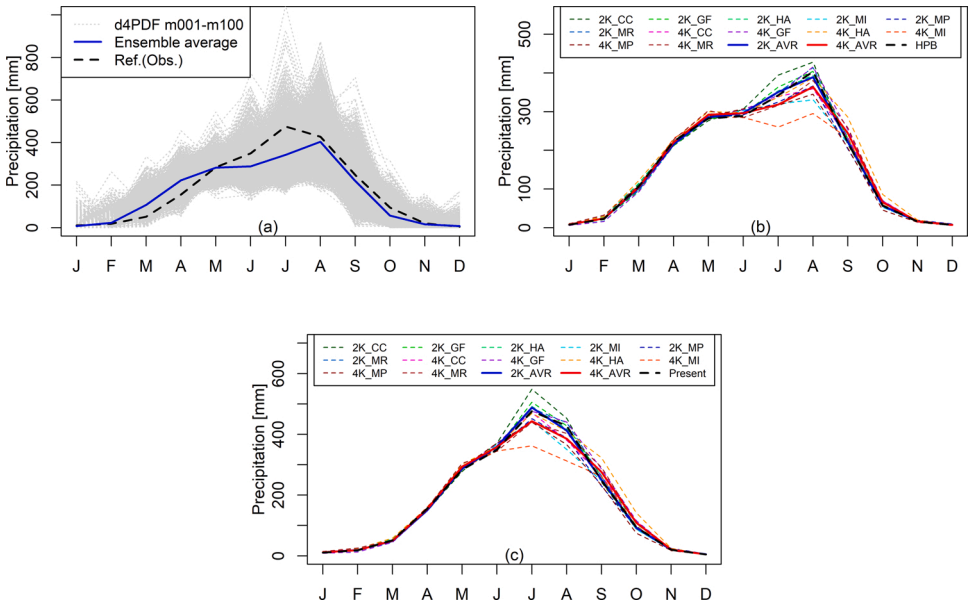

Fig. 5. (a) Comparison of reference data (Observation) and historical experiment of the 100-member ensemble d4PDF basin-averaged monthly precipitation, (b) comparison of basin-averaged monthly precipitation estimated by d4PDF in various climate scenarios in the 2 degree and 4 degree increase experiments and (c) comparison of projected basin-averaged monthly precipitation estimated by using delta change method in various climate scenarios. (HPB is historical data estimated by d4PDF and Present is present value collected from historical observed data).

5.1.2. Actual evapotranspiration projections

Fig. 6**a** shows the mean monthly AET for various climate scenarios obtained from the GCM (d4PDF) prediction. The estimated amount of water transferred to the atmosphere tends to increase as the temperature increases. The monthly delta changes factor obtained by analyzing the GCM data set for +2 K scenarios is ranged from 0.91 to 1.10, for +4 K scenarios is ranged from 0.91 to 1.15.

By using the delta factors obtained by analyzing the d4PDF dataset (Fig. 6a) with the references AET, the AET projection in different climate scenarios was predicted, as shown in Fig. 6**b**. Under the climate projections, the range of increase in mean annual AET compared to the reference (present climate) varies from +0.57 % to +3.78 % for +2 K scenarios and from +4.50 % to +7.94 % for +4 K scenarios. All climate scenarios show the highest amount of AET during April and May in which this period has a high temperature with a moderate precipitation amount. The average pattern of the +2 K climate scenario (2K_AVR) results in a 2.8 average daily value (0.57 % increase from the present climate) and a 2.95 (5.96 % increase) resulted in an average pattern of +4 K climate scenario (4K_AVR).

According to the projected AET, increasing the temperature results in an increase in the potential of water transferred to the atmosphere, leading to fewer water resources available in the basin.

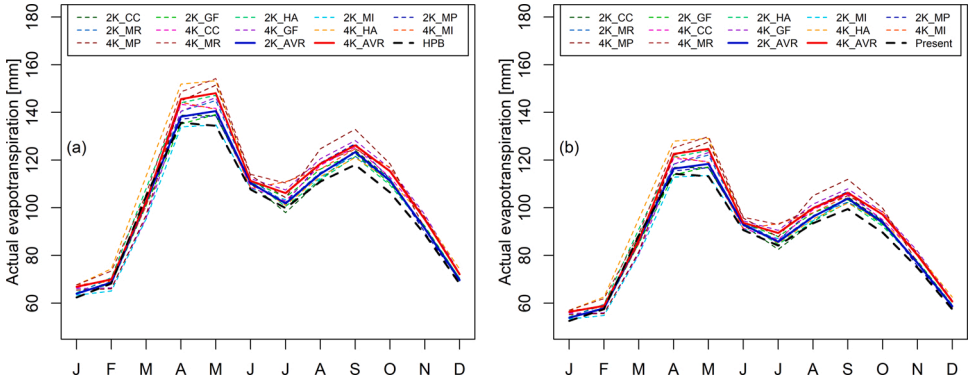

Fig. 6. (a) Comparison of basin-averaged monthly AET in various climate scenarios projected by d4PDF and (b) Comparison of projected basin-averaged monthly AET estimated by using delta change method in various climate scenarios. (HPB is historical data estimated by d4PDF and Present is present value estimated from historical data).

Table 5
Summary of simulation results on annual and seasonal flow at downstream of the Nam Ngum 1 dam (regulated flow) for all simulation scenarios. "Change" is the percent of change from the ND-PS scenario.

Scenario	Wet season		Dry season		Annual		Scenario	Wet season		Dry season		Annual		Scenario	Wet season		Dry season		Annual	
	Flow (m^3/s)	Change (%)	Flow (m^3/s)	Change (%)	Flow (m^3/s)	Change (%)		Flow (m^3/s)	Change (%)	Flow (m^3/s)	Change (%)	Flow (m^3/s)	Change (%)		Flow (m^3/s)	Change (%)	Flow (m^3/s)	Change (%)	Flow (m^3/s)	Change (%)
ND_PS	617.9	–	109.5	–	321.3	–	ED_PS	423.0	−31.5	347.6	217.5	379.0	17.9	FD_PS	425.2	−31.2	347.2	217.1	379.7	18.2
ND_2K_CC	643.5	4.1	109.3	−0.2	331.9	3.3	ED_2K_CC	473.6	−23.4	348.7	218.5	400.7	24.7	FD_2K_CC	474.1	−23.3	347.6	217.4	400.3	24.6
ND_2K_GF	604.5	−2.2	107.6	−1.7	314.6	−2.1	ED_2K_GF	429.1	−30.6	348.3	218.1	382.0	18.9	FD_2K_GF	431.5	−30.2	347.3	217.2	382.3	19.0
ND_2K_HA	606.3	−1.9	110.5	0.9	317.1	−1.3	ED_2K_HA	436.6	−29.3	348.7	218.5	385.3	19.9	FD_2K_HA	439.0	−29.0	347.5	217.4	385.6	20.0
ND_2K_MI	535.1	−13.4	100.0	−8.7	281.3	−12.5	ED_2K_MI	354.8	−42.6	339.8	210.4	346.0	7.7	FD_2K_MI	366.0	−40.8	334.7	205.7	347.8	8.2
ND_2K_MP	540.8	−12.5	103.2	−5.8	285.5	−11.1	ED_2K_MP	362.6	−41.3	341.3	211.7	350.2	9.0	FD_2K_MP	372.4	−39.7	337.0	207.8	351.7	9.5
ND_2K_MR	601.8	−2.6	107.5	−1.8	313.5	−2.5	ED_2K_MR	426.2	−31.0	347.8	217.7	380.5	18.4	FD_2K_MR	428.2	−30.7	347.2	217.1	381.0	18.6
ND_2K_AVR	588.3	−4.8	106.4	−2.8	307.2	−4.4	ED_2K_AVR	412.2	−33.3	346.5	216.5	373.9	16.3	FD_2K_AVR	414.7	−32.9	346.1	216.1	374.7	16.6
ND_4K_CC	570.2	−7.7	105.3	−3.9	299.0	−7.0	ED_4K_CC	388.1	−37.2	345.5	215.6	363.3	13.1	FD_4K_CC	393.1	−36.4	344.2	214.3	364.6	13.5
ND_4K_GF	613.7	−0.7	108.0	−1.3	318.7	−0.8	ED_4K_GF	434.9	−29.6	348.8	218.5	384.7	19.7	FD_4K_GF	438.1	−29.1	347.0	216.9	385.0	19.8
ND_4K_HA	633.8	2.6	117.3	7.1	332.5	3.5	ED_4K_HA	471.6	−23.7	350.6	220.2	401.0	24.8	FD_4K_HA	475.0	−23.1	348.0	217.8	400.9	24.8
ND_4K_MI	468.6	−24.2	96.6	−11.8	251.6	−21.7	ED_4K_MI	313.1	−49.3	323.7	195.7	319.3	−0.6	FD_4K_MI	316.5	−48.8	324.1	196.0	320.9	−0.1
ND_4K_MP	516.5	−16.4	95.7	−12.6	271.0	−15.7	ED_4K_MP	338.9	−45.2	330.9	202.2	334.2	4.0	FD_4K_MP	344.5	−44.3	330.3	201.7	336.2	4.6
ND_4K_MR	569.7	−7.8	107.3	−2.0	300.0	−6.6	ED_4K_MR	389.9	−36.9	345.4	215.4	363.9	13.2	FD_4K_MR	394.7	−36.1	344.5	214.7	365.4	13.7
ND_4K_AVR	561.2	−9.2	105.3	−3.9	295.2	−8.1	ED_4K_AVR	380.1	−38.5	344.1	214.2	359.1	11.8	FD_4K_AVR	384.5	−37.8	343.5	213.8	360.6	12.2

京都大学 KYOTO UNIVERSITY
A Self-archived copy in
Kyoto University Research Information Repository
https://repository.kulib.kyoto-u.ac.jp
京都大学学術情報リポジトリ KURENAI 紅 Kyoto University Research Information Repository

5.2. Climate change and hydropower development impact on river flow

River flow downstream of the NN1 reservoir was used to analyze the impacts of climate change and hydropower development on annual and seasonal flow changes. A comparison of the annual and seasonal flows for all scenarios is summarized in Table 5.

5.2.1. Climate change impact on natural condition flow

A simulation without dams was conducted to assess the impact of climate change on river flow without the impact of dam operation. Fig. 7 shows a comparison of the average monthly flows in various climate scenarios. A comparison between different climate scenarios shows that the change in average annual flow compared to the present climate scenario (ND_PS) ranges from −12.5 % to +3.3 % for +2 K scenarios and from −21.7 % to +3.5 % for +4 K scenarios with a significant difference in magnitude in the wet season (July, August, and September), similar to the projection of precipitation. The average of +2 K (2K_AVR) and +4 K (4K_AVR) climate scenarios showed a decreasing trend in the annual river flow of −4.4 % and −8.1 %, respectively.

5.2.2. Climate change impact on Nam Song water diversion

To predict the amount of water diversion in different climate scenarios, we adopted the ratio between the simulated flow in the present climate condition and the discharge of the diversion record and then applied the ratio with the simulated river discharge for each climate scenario. The diverted water discharge is limited to the maximum diversion capacity.

Fig. 8**a** presents the change in mean monthly water availability at the diversion headwork (Nam Song River) in different climate scenarios in which the mean annual flow varies from −7.5 % to + 6.3 % for +2 K scenarios and from −15.7 % to + 8.1 % for +4 K scenarios compared with present climate scenarios.

Fig. 8**b** presents the change in mean monthly water diversion from the Nam Song at diversion headwork to the NN1 reservoir in different climate scenarios, where the mean annual diversion discharge varied from −4.5 % to +2.2 % for +2 K scenarios and from −9.6 % to +6.1 % for +4 K scenarios compared with the present climate scenarios.

According to the simulation results, climate change has a less significant effect on the total amount of water diversion from the Nam Song River to the NN1 reservoir compared to the change in water availability at the diversion headwork (inflow of the Nam Song dam). For example, in the case of the 4K_MI climate scenario (the greatest reduction of river flow), the reduction of water transfer to the NN1 reservoir is only a 1.5 % reduction from the NN1 reservoir total inflow compared to the present climate scenario with ED conditions (ED_PS).

5.2.3. Climate change impact on river flow with existing dam condition

Fig. 9**a** describes the impact of climate change on the inflow of the NN1 reservoir with the ED conditions. The change in the annual inflow ranges from −8.3 % to +5.9 % for +2 K scenarios and from −16.7 % to +6.5 % for +4 K scenarios compared to the present climate scenario (ED_PS). To assess the combined effect of climate change and dam development, the degree of change in the river flow was compared with the natural flow condition (ND_PS), and a range of change in the mean annual inflow from +0.3 % to +28.2 % was found. A significant change in seasonal flow (inflow of NN1) due to upstream dam development in different climate scenarios, compared with natural flow conditions (ND_PS), varies from +74.1 % to +117.3 % in the dry season and −18 % to +8.2 % in the wet season. A significant alteration in the seasonal inflow of NN1 is mainly due to the regulation of a large storage dam, such as NN2, with an effective storage capacity of 2617 mcm.

Fig. 9**b** describes the impact of climate change on the regulated flow of the NN1 reservoir with inflow from the existing upstream dam condition. The change in the annual regulated flow downstream of the NN1 reservoir for different climate scenarios ranged from −8.7 % to +5.7 % for +2 K scenarios and from −15.8 % to +5.8 % for +4 K scenarios compared to the present climate scenario (ED_PS).

The effect of the NN1 reservoir regulation with a large effective storage of 4714 mcm was assessed by comparing the seasonal flow change between the predicted inflow (Fig. 9a) and regulated flow (Fig. 9b) for each climate condition. The simulation result shows a 49.0 − 22.9 % reduction in the wet season and a 44.2 − 56.1 % increase in the dry season.

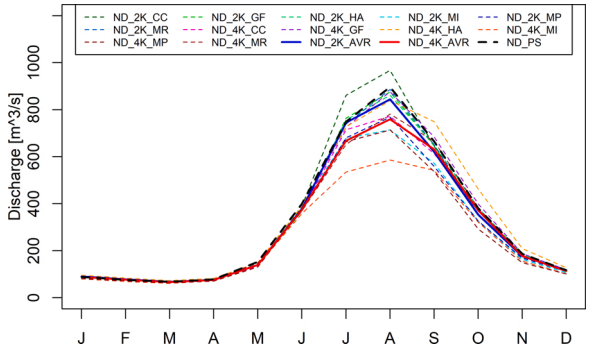

Fig. 7. Mean monthly projected river flow at the Nam Ngum 1 dam in different climate scenarios without dam (Unregulated flow).

京都大学 KYOTO UNIVERSITY
A Self-archived copy in
Kyoto University Research Information Repository
https://repository.kulib.kyoto-u.ac.jp
京都大学学術情報リポジトリ KURENAI 紅 Kyoto University Research Information Repository

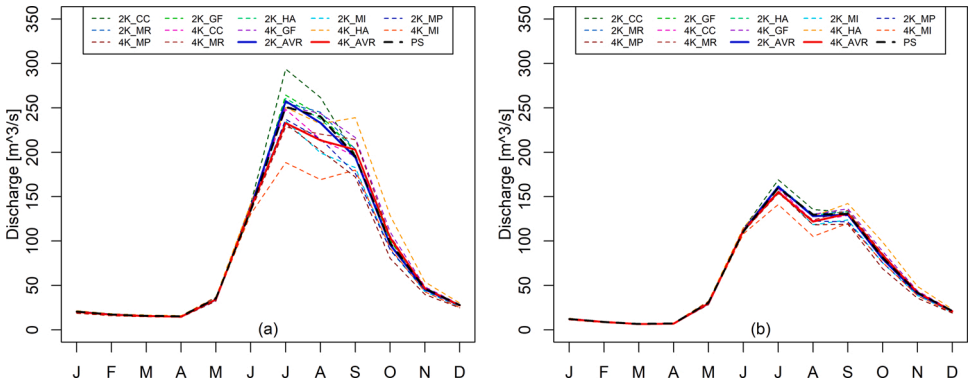

Fig. 8. Mean monthly projected flow at the Nam Song diversion dam in different climate scenarios (a) inflow of the Nam Song diversion dam and (b) diversion discharge to the Nam Ngum 1 reservoir.

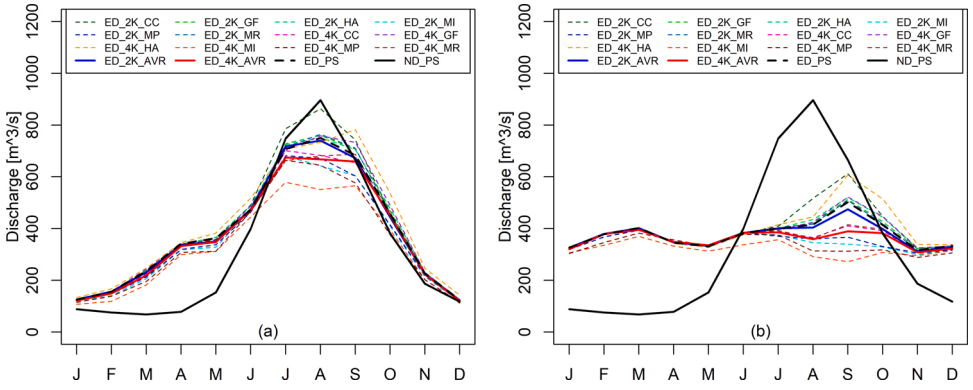

Fig. 9. Comparison of mean monthly river flow between base line (present climate without dam, ND_PS) and different climate scenarios with existing dam development stage (a) inflow of the Nam Ngum 1 reservoir and (b) regulated flow to downstream of the Nam Ngum reservoir.

5.2.4. Climate change impact on river flow with future dam condition

Fig. 10**a** shows the impact of climate change on the inflow of the NN1 reservoir with the regulated flow from the future upstream dam conditions (NS_DV, NL, NN2, and NN3). The change in the annual inflow of the NN1 reservoir for different climate scenarios ranged from −8.0 % to +5.6 % for +2 K scenarios and from −16.2 % to +6.3 % for +4 K scenarios compared with the present climate scenario (FD_PS). The inflow of the NN1 reservoir becomes more stable (a slight decrease in seasonal variation) due to an increase in the regulated storage of the upstream dams. An additional power station, NN3, with an effective storage of 1070 mcm, was considered in this simulation. To assess the impact of NN3 regulation on the inflow of NN1, the simulated inflow for FD development conditions

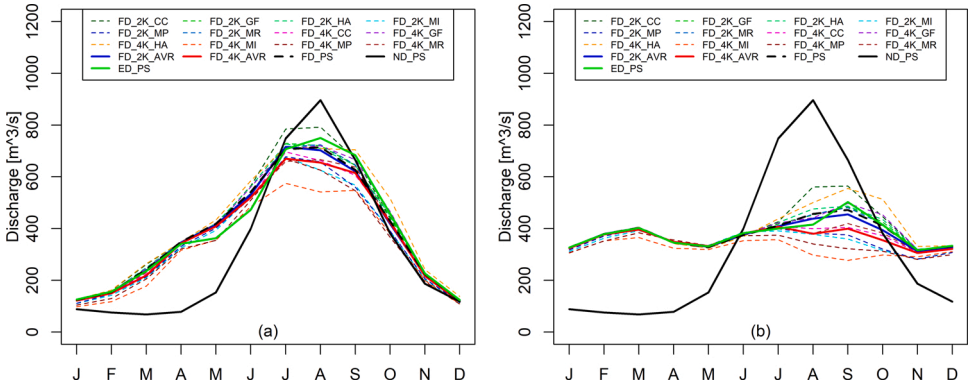

Fig. 10. Comparison of mean monthly river flow among present climate without dam (ND_PS), present climate with existing dam (ED_PS) and different climate scenarios with future dam development stage (a) inflow of the Nam Ngum 1 reservoir and (b) regulated flow to downstream of the Nam Ngum reservoir.

京都大学 KYOTO UNIVERSITY
A Self-archived copy in
Kyoto University Research Information Repository
https://repository.kulib.kyoto-u.ac.jp
京都大学学術情報リポジトリ KURENAI 紅 Kyoto University Research Information Repository

(Fig. 10a) was compared with the ED condition (Fig. 9a) for each climate scenario. The results show that there is a slight reduction of 0.2 − 2.6 % in the wet season inflow and a slight increase of 2.4 − 5.3 % in the dry season inflow of the NN1 reservoir.

Fig. 10**b** shows the impact of climate change on the regulated flow of the NN1 reservoir downstream with FD conditions. The change in the annual river flow downstream of the NN1 reservoir for different climate scenarios ranged from −8.4 % to +5.4 % for +2 K scenarios and from −15.5 % to +5.6 % for +4 K scenarios compared with the present climate scenario (FD_PS). The primary change in seasonal river flow due to dam development in different climate scenarios, compared with natural flow conditions (ND_PS) downstream of the NN1 reservoir, varied from −48.8 % to −23.1 % in the wet season and +196.0 % to +217.8 % in the dry season.

To assess the impact of the NN3 operation on the regulated flow of NN1, the regulated flow under the FD condition (Fig. 10b) is compared to the river flow under the ED condition (Fig. 9b) for each climate scenario. The results show that there is no primary change in the regulated flow from the NN1 reservoir to the downstream because the regulated potential of NN3 (effective storage of 1070 mcm) is approximately only 9.0 % (range from 8.2%–10.4%) of the mean predicted total inflow of NN1 for different climate scenarios with FD conditions. This agrees with Meema et al. (2020) that major large-scale hydropower dams have already been developed, which can regulate most river flows in the basin.

By comparing the individual effects of climate change and dam development with the natural flow condition (ND_PS), the changing climate has a primary effect in terms of the total amount of water availability (mean annual river flow) due to the combined effect of precipitation change and AET increase. A significant effect occurs during the wet season due to a change in the magnitude of precipitation, leading to a change in river flow. Only a slight change in seasonal flow driven by climate change was observed in this study.

Dam development in the basin has a primary effect in terms of seasonal flow variation due to regulation using storage. Furthermore, not only a primary change in seasonal flow but dam development with a river diversion type from another catchment results in increasing of mean annual river flow as well. The simulation results demonstrate that the large-scale dam reservoir, which can control a large volume of water in the basin, plays an important role in water resource management.

5.3. *Link between projected precipitation, evaporation, inflow, and regulated flow*

The model includes soil and bedrock aquifers that respond to the natural storage of the basin. During the dry season, the amount of precipitation is lower than that of AET, and the storage is the primary contributor to the basin. Although some effective rainfall occurs (precipitation > AET) during the beginning of the wet season (May and June), most rainwater infiltrates into the aquifers. Therefore, the hydrograph of river flow (Fig. 7) shows a minor difference during these periods.

The highest amount of precipitation occurs in July and August, and effective rainfall is sufficient to become surface flow. The magnitude of river flow is dependent on the amount of projected precipitation, resulting in a primary difference in the river flow hydrograph (as shown in Fig. 7).

In September and October, the storages become fully filled from the previous months, and most effective rainwater becomes surface runoff. A combination of groundwater and surface flow results in a significantly higher difference in river flow compared to precipitation.

The major difference in regulated flow among the scenarios was due to the spillage water. In this study, we assumed that the operation follows the present operation. Therefore, during the dry season, including the beginning of wet seasons such as June and July, the amount of reservoir inflow can be controlled by the reservoir storage (current storage; S_t <= maximum storage; S_{max}). Therefore, the comparison of regulated flow for various scenarios is quite similar (as shown in Figs. 9 and 10). During the mid to late wet seasons (August to October), significant spilling occurs ($S_t > S_{max}$) when river discharge has an increasing trend, leading to a significant difference in regulated flow during this period (as shown in Figs. 9 and 10).

Although a larger difference in precipitation was observed in July and August, the primary difference in regulated flow from NN1 was found in August to October due to the storage capacity (regulated capacity) of the reservoirs. In this study, the hydrological

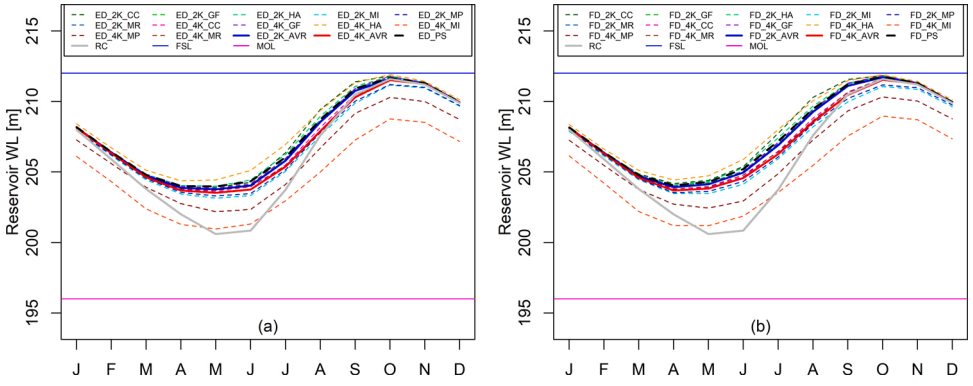

Fig. 11. (a) comparison of mean monthly reservoir water level for different climate scenarios with existing dam condition and (b) comparison of mean monthly reservoir water level between present climate scenario with existing dam (ED_PS) and different climate scenarios with future dam condition. (RC: rule curve, FSL: full supply level and MOL: minimum operation level).

京都大学 KYOTO UNIVERSITY
A Self-archived copy in
Kyoto University Research Information Repository
https://repository.kulib.kyoto-u.ac.jp
京都大学学術情報リポジトリ KURENAI 紅 Kyoto University Research Information Repository

residence time (HRT) of the NN1, NN2 and NN3 reservoirs for the present climate scenarios with FD condition are 0.39, 0.46 and 0.41 year respectively (HRT [year] = effective storage capacity [mcm] / inflow [mcm/year]). Conversely, when the HRT decreases, the regulated hydrograph is closer to the inflow hydrograph.

5.4. Climate change impact on reservoir water level and water spillage

Fig. 11**a** presents a comparison of the mean monthly water level of the NN1 reservoir in different climate scenarios with ED conditions. A change of mean water level for different climate scenarios compared with present climate scenarios (ED_PS) is varied from −0.63 to + 0.12 m for +2 K scenarios and from −2.86 to + 0.41 m for +4 K scenarios. For the average climate scenarios such as 2K_AVR and 4K_AVR, the reduction in mean reservoir water level is 0.12 and 0.34 m, respectively.

Fig. 11**b** presents a comparison of the mean monthly water level of the NN1 reservoir in different climate scenarios with FD conditions. The tendency of the mean monthly reservoir water level is quite similar to that of the ED condition (Fig. 11a), but the trend is slightly increased. By using the same operation pattern, more stable inflow (increase in the dry season flow and decrease in the wet season) due to an increase in the regulation capacity of the upstream dam results in slightly higher water levels in the reservoir, resulting in a 0.18 − 0.36 m increase in mean reservoir water level compared with the ED condition for each climate scenario.

Table 6 summaries the mean annual reservoir water and the total amount of water spillage from the NN1 reservoir in different simulation scenarios. The mean annual amount of water spillage for all simulation scenarios is ranged from 0 to 921.6 mcm. For each dam development condition, the mean annual water spillage trends to increase when the mean reservoir water level increases.

To assess the effect of dam development on water spills from the NN1 reservoir, the amount of water spillage for each climate scenario between the ED and FD conditions was compared. It was revealed that although all climate scenarios in FD result in an increase in mean water level compared with ED, some climate scenarios result in a reduction of a water spill. This demonstrated that the amount of water spillage is not only a function of the water level but also other factors. For example, in the case 4K_MR, Although the mean water level in FD has a 0.2 m higher than ED, the water spillage is reduced by 42.0 %. Because the water level in FD is generally higher than ED during the period without spills (spills usually occur in September and October) and the regulated flow from the upstream in the FD condition is more appropriate for power generation, most water is used to generate power through the turbines, leading to less water spillage through the spillway.

The water level of the NN1 Reservoir seems to have less fluctuation when there are more reservoirs upstream because of its regulated flow, which tends to increase the NN1 inflow in the dry season and decrease in the wet season.

The water spill is the amount of water released through the spillway without generating electricity when the current reservoir storage exceeds the maximum storage. Thus, to use water effectively, the operation of the reservoir should be considered to avoid the water spillage.

5.5. Climate change impact on hydropower production

The hydrologic impact on hydropower production was analyzed considering the overall effect on climate change and upstream dam development. The simulation results of the mean annual energy production for different simulation scenarios are listed in Table 7.

Fig. 12**a** presents a comparison of the mean monthly energy product of the NN1 power station in different climate scenarios with the ED development conditions. Under projected climate scenarios, the difference in mean annual energy production compared to the present climate (ED_PS) varies from –8.4 % to +1.9 % for +2 K scenarios and from −19.5 % to +2.8 % for +4 K scenarios. Its reduction in energy production due to a reduction in inflow to the reservoir and a decrease in reservoir water level (leading to generated hydraulic head reduction) results in decreased energy production.

Table 6
Summary of simulation result on the mean annual reservoir water and the total amount of water spill from the Nam Ngum 1 reservoir for different climate scenarios with the existing (ED) and future (FD) dam development conditions.

Existing dams (ED)	Water level (m)	Spill (mcm)	Future dams (FD)	Water level (m)	Spill (mcm)
ED_PS	207.5	348.1	FD_PS	207.8	399.4
ED_2K_CC	207.6	856.0	FD_2K_CC	208.0	911.6
ED_2K_GF	207.5	423.1	FD_2K_GF	207.8	458.7
ED_2K_HA	207.6	438.0	FD_2K_HA	207.9	541.5
ED_2K_MI	206.9	68.0	FD_2K_MI	207.1	85.2
ED_2K_MP	207.0	82.2	FD_2K_MP	207.2	84.7
ED_2K_MR	207.4	403.7	FD_2K_MR	207.8	414.2
ED_2K_AVR	207.4	310.8	FD_2K_AVR	207.7	308.9
ED_4K_CC	207.3	184.0	FD_4K_CC	207.5	146.0
ED_4K_GF	207.5	478.7	FD_4K_GF	207.8	538.9
ED_4K_HA	207.9	855.4	FD_4K_HA	208.2	921.6
ED_4K_MI	204.7	0.0	FD_4K_MI	204.9	0.0
ED_4K_MP	206.1	19.8	FD_4K_MP	206.3	59.1
ED_4K_MR	207.3	215.4	FD_4K_MR	207.5	124.9
ED_4K_AVR	207.2	151.9	FD_4K_AVR	207.4	104.2

京都大学 KYOTO UNIVERSITY
A Self-archived copy in
Kyoto University Research Information Repository
https://repository.kulib.kyoto-u.ac.jp
京都大学学術情報リポジトリ KURENAI 紅 Kyoto University Research Information Repository

Table 7
Summary of simulation result on the mean annual energy production of the Nam Ngum 1 power station for different climate scenarios with the existing (ED) and future (FD) dam development conditions. "Change" is the percent of change from the ED_PS scenario.

Scenario	Energy (GWh)	Change (%)	Scenario	Energy (GWh)	Change (%)
ED_PS	1080.6	–	FD_PS	1085.7	0.5
ED_2K_CC	1101.5	1.9	FD_2K_CC	1104.8	2.2
ED_2K_GF	1081.5	0.1	FD_2K_GF	1087.7	0.7
ED_2K_HA	1093.6	1.2	FD_2K_HA	1092.1	1.1
ED_2K_MI	989.8	−8.4	FD_2K_MI	998.1	−7.6
ED_2K_MP	1003.6	−7.1	FD_2K_MP	1013.4	−6.2
ED_2K_MR	1077.0	−0.3	FD_2K_MR	1086.6	0.6
ED_2K_AVR	1064.6	−1.5	FD_2K_AVR	1075.4	−0.5
ED_4K_CC	1040.9	−3.7	FD_4K_CC	1055.2	−2.3
ED_4K_GF	1084.9	0.4	FD_4K_GF	1087.9	0.7
ED_4K_HA	1110.8	2.8	FD_4K_HA	1110.5	2.8
ED_4K_MI	869.6	−19.5	FD_4K_MI	877.7	−18.8
ED_4K_MP	940.4	−13.0	FD_4K_MP	946.8	−12.4
ED_4K_MR	1039.5	−3.8	FD_4K_MR	1059.7	−1.9
ED_4K_AVR	1029.1	−4.8	FD_4K_AVR	1044.1	−3.4

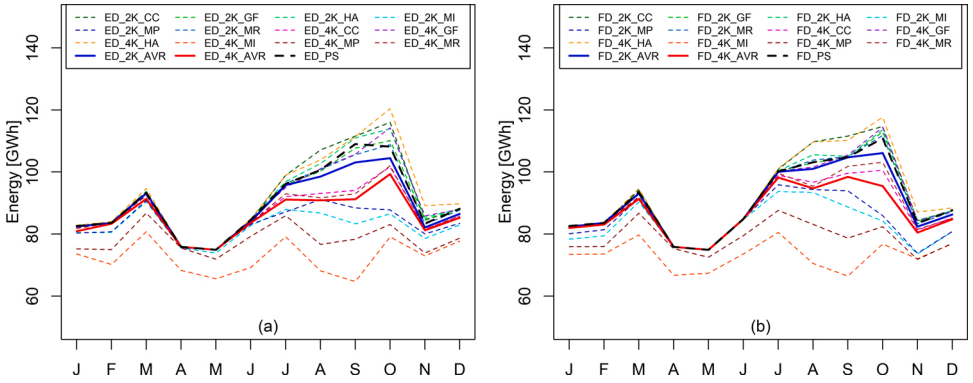

Fig. 12. (a) Comparison of energy production for NN1 power station with existing dam stage in different climate scenarios and (b) Comparison of energy production for NN1 power station with future dam stage in different climate scenarios.

Fig. 12**b** illustrates a comparison of the mean monthly energy product of the NN1 power station in different climate scenarios with the FD development conditions. The change in mean annual energy production from the present climate (FD_PS) for different projected climate scenarios is quite similar to a change in the ED development conditions. To demonstrate the effect of upstream cascade dam development on energy production of the NN1 power station, the mean monthly energy between the existing (Fig. 12a) and future (Fig. 12b) dam development conditions were compared for each climate scenario. Under the FD development level, the annual energy production of the NN1 power station has a slightly increasing trend due to more upstream reservoirs in operation.

The construction of upstream cascade dams improves the stabilization between the wet and dry seasons of inflow to the NN1 reservoir, leading to an improvement in the reservoir water level and thus increasing the potential for power generation and total energy production. However, a general trend (2K_AVR and 4K_AVR) seems to indicate a reduction in the annual energy product when the projected temperature is increased.

5.6. Climate change impact on water loss from the reservoir

The mean monthly evaporation rate from the water body was placed at the reservoirs to account for the net amount of water loss due to evaporation from the water surface of the reservoirs. The differences in water loss from the NN1 reservoir for the different simulation scenarios are summarized in Table 8.

Fig. 13**a** presents a comparison of the mean monthly amount of water loss from the NN1 reservoir in different climate scenarios with the ED development conditions. The amount of water loss due to evaporation in different climate scenarios varies from 9.2 % to 13.4 % for +2 K scenarios and from 24.5 % to 35.6 % for +4 K scenarios compared to the present climate with the ED development stage (ED_PS). Although the evaporation loss rates in November and December were significantly lower than those in March and April (as shown in Fig. 13c), the net amount of water loss was quite similar (as shown in Fig. 13a). The operation pattern tries to maintain the water in the reservoir at a high level at the end of the rainy season and the beginning of the dry season, leading to an increase in free water surface area, which results in a high amount of water loss.

京都大学 KYOTO UNIVERSITY
A Self-archived copy in
Kyoto University Research Information Repository
https://repository.kulib.kyoto-u.ac.jp
京都大学学術情報リポジトリ KURENAI 紅 Kyoto University Research Information Repository

Table 8
Summary of simulation result on the mean annual water loss due to evaporation from the Nam Ngum 1 reservoir for different climate scenarios with the existing (ED) and future (FD) dam development conditions. "Change" is the percent of change from the ED_PS scenario.

Existing dams (ED)	Loss (mcm)	Change (%)	Future dams (FD)	Loss (mcm)	Change (%)
ED_PS	289.2	–	FD_PS	290.8	0.5
ED_2K_CC	323.7	11.9	FD_2K_CC	326.0	12.7
ED_2K_GF	323.6	11.9	FD_2K_GF	325.5	12.6
ED_2K_HA	326.0	12.7	FD_2K_HA	327.7	13.3
ED_2K_MI	315.8	9.2	FD_2K_MI	316.9	9.6
ED_2K_MP	325.4	12.5	FD_2K_MP	326.8	13.0
ED_2K_MR	328.1	13.4	FD_2K_MR	330.1	14.1
ED_2K_AVR	324.3	12.1	FD_2K_AVR	326.1	12.7
ED_4K_CC	371.3	28.4	FD_4K_CC	373.1	29.0
ED_4K_GF	384.7	33.0	FD_4K_GF	386.9	33.8
ED_4K_HA	380.8	31.7	FD_4K_HA	382.4	32.2
ED_4K_MI	360.1	24.5	FD_4K_MI	361.2	24.9
ED_4K_MP	380.5	31.6	FD_4K_MP	381.9	32.0
ED_4K_MR	392.2	35.6	FD_4K_MR	394.0	36.2
ED_4K_AVR	382.7	32.3	FD_4K_AVR	384.3	32.9

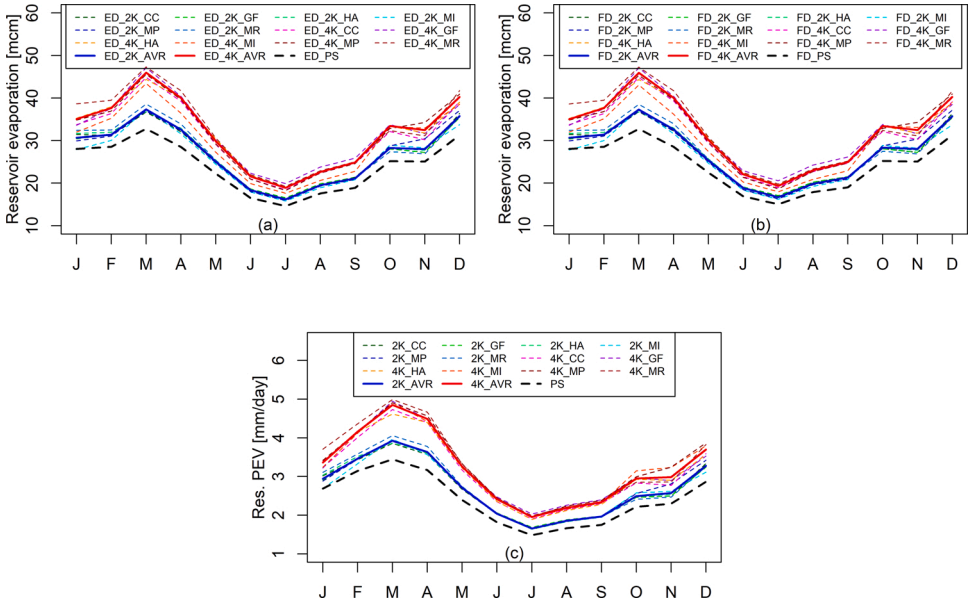

Fig. 13. (a) mean monthly net amount of water loss from the NN1 reservoir due to evaporation in different climate scenarios for existing dam development stage. (b) mean monthly net amount of water loss from the NN1 reservoir due to evaporation in different climate scenarios for future dam development stage. (c) mean monthly evaporation rate from water body in different climate scenarios.

Fig. 13**b** presents a comparison of the mean monthly amount of water loss from the NN1 reservoir in different climate scenarios with the FD development conditions. The tendency of water loss from the reservoir in different climate scenarios compared to the present climate (FD_PS) is quite similar to the ED development conditions. By comparing the simulation results under different climate scenarios between the FD condition (Fig. 13b) and the ED condition (Fig. 13a) to assess the impact of FD development on the projected amount of water loss from the NN1 reservoir, there is a slight increase in actual water loss. As the water level increases, the reservoir water surface area increases, which results in an additional amount of water loss due to evaporation.

The amount of water loss from the reservoir in the present (ED_PS) is approximately 2.4 % of the total inflow of the NN1 reservoir. However, under the projected climate scenarios, the amount of water loss from the NN1 reservoir due to evaporation will increase to approximately 2.7 % and 3.2 % of the present mean annual inflow for the 2 K and 4 K temperature increase scenarios, respectively (2K_AVR and 4K_AVR). Assume that the total amount of water loss due to evaporation can be used to utilize the hydropower, an approximately 3.6 and 9.4 GW h/year of additional energy production for the NN1 power station will be lost when the temperature increases by 2 K and 4 K, respectively (2K_AVR and 4K_AVR).

京都大学 KYOTO UNIVERSITY
A Self-archived copy in
Kyoto University Research Information Repository
https://repository.kulib.kyoto-u.ac.jp
京都大学学術情報リポジトリ KURENAI 紅 Kyoto University Research Information Repository

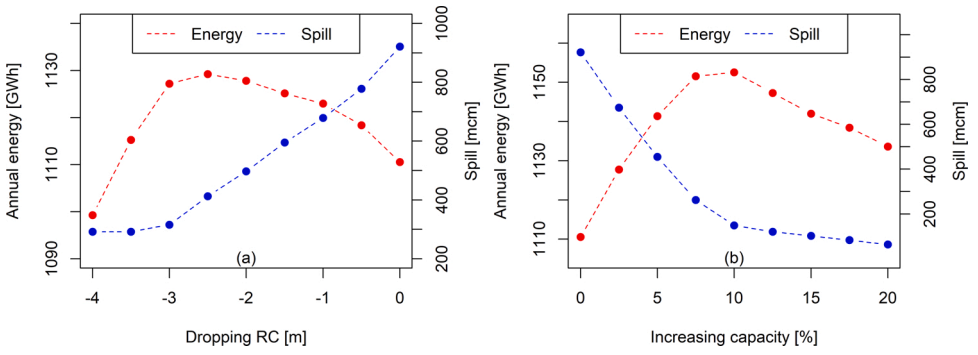

Fig. 14. (a) A relationship among dropping rule curve level, water spill and annual energy output of the NN 1 power station for FD_4K_HA. (b) A relationship among increasing installed capacity, water spill and annual energy output of the NN 1 power station for FD_4K_HA.

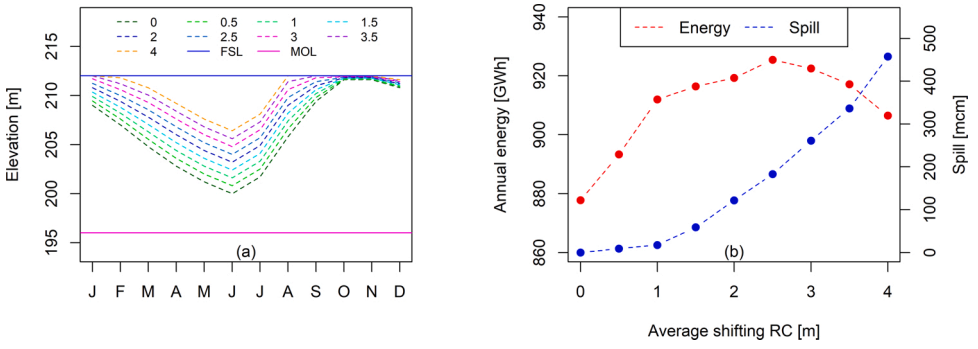

Fig. 15. (a) shifting elevation of the NN1 rule curve in different levels, the number shows the average shifting level of the rule curve from the existing in meter and (b) the relationship among annual energy, water spill and the shifting rule curve.

5.7. Reservoir operation strategy to cope with climate change

As hydropower production is strongly related to inflow, the power generation for the NN1 power station could vary significantly owing to large variations in inflow projections. To mitigate variability, implementing strategies such as changing the existing operation is necessary. Fig. 14 shows the implementation of reservoir operation of the NN1 reservoir for the increasing trend of inflow (for example, the 4K_HA scenario). Fig. 14**a** shows the implementation by dropping the level of the NN1 rule curve to avoid a spill. By decreasing the rule curve to a lower level, the results show that water spills tend to decrease and energy production tends to increase. Although decreasing the level of the rule curve over 2.5 m results in a higher reduction of the water spill, the head is reduced, resulting in less power output. The maximum increase in energy output has resulted when dropping the rule curve by 2.5 m with a 1.7 % increase in energy production compared to the existing rule curve (dropping 0 m). Fig. 14**b** shows the implementation by increasing the installed power capacity. It is possible that in terms of the future inflow trend has increased, stakeholders can consider installing more capacity to utilize additional water to generate more power. Engineering design and construction processes are also required. Furthermore, by increasing the power capacity, the implementation cost should be considered against the benefit of an increase in energy production. By increasing the capacity (with the existing rule curve), the results show that water spills tend to decrease and energy production tends to increase. Although the water spillage is decreased when the capacity is increased above 10 %, it results in less energy output because a large amount of water is discharged downstream, which results in a reduction in the water level in the reservoir (reduction head), leading to less power generation. The maximum increase in energy output was observed when the capacity was increased by 10 %, with a 3.8 % increase in energy production compared to the existing capacity.

Fig. 15 shows the implementation of reservoir operation of the NN1 reservoir by changing the rule curve for the decreasing trend of inflow (for example, the FD_4K_MI scenario). Fig. 15**a** shows the shifting elevation of the NN1 rule curve at different levels. Fig. 15**b** shows the implementation of the NN1 reservoir by shifting the rule curve to a higher level. By shifting the rule curve (as shown in Fig. 15a), a higher hydraulic head is provided because higher reservoir water levels result in increased energy production. As a result of the higher water level, the water spillage tended to increase. Although the water level in the reservoir is increased when shifting the rule curve with an average shift elevation higher than 2.5 m, the energy output tends to decrease because of the higher water spill. The maximum increase in energy output has resulted when shifting the rule curve of the NN1 reservoir by 2.5 m on average with a 5.4 % increase in energy production compared to the rule curve.

京都大学 KYOTO UNIVERSITY
A Self-archived copy in
Kyoto University Research Information Repository
https://repository.kulib.kyoto-u.ac.jp
京都大学学術情報リポジトリ KURENAI 紅 Kyoto University Research Information Repository

6. Conclusion

A change in long-term river flow projection covers a wide range dominated mainly by the difference in precipitation projections. The mean climate projections of the +2 K and +4 K scenarios (2K_AVR and 4K_AVR) show a slight decrease in the mean annual river flow. Although climate change has a primary effect on river flow in total annual amount, the impact on seasonal flow change is quite low compared to the effect of dam development. The effect of dam development shows a significant reduction in seasonal flow variation downstream of the NN1 reservoir (regulated flow) in all climate scenarios compared to the natural flow condition (ND). At the FD stage, all climate scenarios show a distinct trend of change in seasonal flow compared to the ED stage, with a slight increase in the dry season and a slight decrease in the wet season due to an additional regulated storage of the under-construction dam (NN3).

The estimation of energy production of the NN1 power station under climate projections shows a large variation in the mean annual energy output due to the uncertainty of river flow projections in different climate scenarios. At the FD stage, the annual energy production has a slightly increasing trend compared to the ED development stage because of the regulated flow from the storage of the upstream cascade dam.

With an increase in temperature projections, the NNBR seems to face a decreasing trend in future precipitation. A combination of precipitation reduction and high temperatures resulted in a reduction in river flow and hydropower production. Without any implementation, the existing operation will lead to a loss in the annual energy production. Thus, adaptive implementations are necessary to mitigate the impact of climate change on long-term hydropower generation. The rule curve needs to be effectively managed to optimize hydropower production while other related purposes such as downstream flood risk, water demand deficit, ecosystems, and social vulnerability are minimized.

Based on our approach for this study, there are some limitations. First, by using the delta method to project climate variables, there is a lack of change in the variability and spatial patterns of climate. A GCM downscale including a bias correction process might be required to access the spatial distribution and variability of the projected climate.

Second, this study assumed that the hydrologic variables that have an influence on river flow projection (including basin land cover) do not change. In future studies, land use change and upstream water use (e.g., for irrigation) should be considered.

The operation of a large-scale dam with a large storage capacity can play a primary role in water resource management in the river basin. To improve the efficiency of reservoir operation, the consideration of forecast information should be carried out. However, the hydrological forecast has significant uncertainties, and it is difficult to predict future conditions perfectly. Nohara et al. (2016) applied the ensemble prediction technique to support preliminary operation of the reservoir. The information including the possible conditions and the uncertainty of prediction can be important for more effective decision strategy for the reservoir real-time operation.

Author statement

Thatkiat Meema: Conceptualization, Methodology, Analysis, Software, Visualization, Writing - Original Draft.
Yasuto Tachikawa: Supervision, Conceptualization, Methodology, Writing - Review & Editing.
Yutaka Ichikawa: Conceptualization, Methodology.
Kazuaki Yorozu: Conceptualization, Resources.

Declaration of Competing Interest

The authors report no declarations of interest.

Acknowledgements

We thank Mr. Bounhome Kimmany, Faculty of Water Resources, National University of Laos, for providing the hydrologic data in the Nam Ngum River basin. This study was supported by the Integrated Research Program for Advancing Climate Models (TOUGOU) Grant Number JPMXD0717935498 from the Ministry of Education, Culture, Sports, Science and Technology (MEXT), Japan. This study used d4PDF produced with the Earth Simulator jointly by science programs (SOUSEI, TOUGOU, SI-CAT, DIAS) of MEXT. This dataset was collected and provided under the Data Integration and Analysis System (DIAS), which has been developed and operated by MEXT, Japan.

Appendix A. Supplementary data

Supplementary material related to this article can be found, in the online version, at doi:https://doi.org/10.1016/j.ejrh.2021.100856.

京都大学 KYOTO UNIVERSITY
A Self-archived copy in
Kyoto University Research Information Repository
https://repository.kulib.kyoto-u.ac.jp
京都大学学術情報リポジトリ KURENAI 紅 Kyoto University Research Information Repository

References

ADB, 2019. Lao People's Democratic Republic Energy Sector Assessment, Strategy, and Road Map.
Ayers, J., Ficklin, D.L., Stewart, I.T., Strunk, M., 2016. Comparison of CMIP3 and CMIP5 projected hydrologic conditions over the Upper Colorado River Basin. Int. J. Climatol. 36, 3807–3818. https://doi.org/10.1002/joc.4594.
Beyene, T., Lettenmaier, D.P., Kabat, P., 2010. Hydrologic impacts of climate change on the Nile River Basin: implications of the 2007 IPCC scenarios. Clim. Change 100, 433–461. https://doi.org/10.1007/s10584-009-9693-0.
Blackshear, B., Crocker, T., Drucker, E., Filoon, J., Knelman, J., Skiles, M., 2011. Hydropower Vulnerability and Climate Change - A Framework for Modeling the Future of Global Hydroelectric Resources. Middlebury College Environmental Studies Senior Seminar.
Bourke, R.H., Garrett, R.P., 1987. Sea ice thickness distribution in the Arctic Ocean. Cold Reg. Sci. Technol. 13, 259–280. https://doi.org/10.1016/0165-232X(87)90007-3.
Carvajal, P.E., Anandarajah, G., Mulugetta, Y., Dessens, O., 2017. Assessing uncertainty of climate change impacts on long-term hydropower generation using the CMIP5 ensemble—the case of Ecuador. Clim. Change 144, 611–624. https://doi.org/10.1007/s10584-017-2055-4.
Endo, H., Kitoh, A., Mizuta, R., Ishii, M., 2017. Future changes in precipitation extremes in East Asia and their uncertainty based on large ensemble simulations with a high-resolution AGCM. Sci. Online Lett. Atmos. 13, 7–12. https://doi.org/10.2151/sola.2017-002.
Fan, J.-L., Hu, J.-W., Zhang, X., Kong, L.-S., Li, F., Mi, Z., 2020. Impacts of climate change on hydropower generation in China. Math. Comput. Simul. 167, 4–18. https://doi.org/10.1016/j.matcom.2018.01.002.
Fujita, M., Mizuta, R., Ishii, M., Endo, H., Sato, T., Okada, Y., Kawazoe, S., Sugimoto, S., Ishihara, K., Watanabe, S., 2019. Precipitation changes in a climate with 2-K surface warming from large ensemble simulations using 60-km global and 20-km regional atmospheric models. Geophys. Res. Lett. 46, 435–442. https://doi.org/10.1029/2018GL079885.
Grijsen, J., Patel, H., 2014. Understanding the impact of climate change on hydropower: the case of Cameroon understanding the impact of climate change on hydropower: the case of Cameroon climate risk assessment for hydropower generation in Cameroon. Africa Energy Pract. 151.
Hamlet, A.F., Lee, S.-Y., Mickelson, K.E.B., Elsner, M.M., 2010. Effects of projected climate change on energy supply and demand in the Pacific Northwest and Washington State. Clim. Change 102, 103–128. https://doi.org/10.1007/s10584-010-9857-y.
Hamududu, B., Killingtveit, A., 2012. Assessing climate change impacts on global hydropower. Energies 5, 305–322. https://doi.org/10.3390/en5020305.
Hanittinan, P., Tachikawa, Y., Ram-Indra, T., 2020. Projection of hydroclimate extreme indices over the Indochina region under climate change using a large single-model ensemble. Int. J. Climatol. 40, 2924–2952. https://doi.org/10.1002/joc.6374.
Hawkins, E., Sutton, R., 2009. The potential to narrow uncertainty in regional climate predictions. Bull. Am. Meteorol. Soc. 90, 1095–1108. https://doi.org/10.1175/2009BAMS2607.1.
Hay, L.E., Wilby, R.L., Leavesley, G.H., 2000. A comparison of delta change and downscaled GCM scenarios for three mountainous basins in the United States. J. Am. Water Resour. Assoc. 36, 387–397. https://doi.org/10.1111/j.1752-1688.2000.tb04276.x.
Hibino, K., Takayabu, I., Wakazuki, Y., Ogata, T., 2018. Physical responses of convective heavy rainfall to future warming condition: case study of the Hiroshima event. Front. Earth Sci. 6, 1–9. https://doi.org/10.3389/feart.2018.00035.
Hirahara, S., Ishii, M., Fukuda, Y., 2014. Centennial-scale Sea Surface Temperature Analysis and its uncertainty. J. Clim. 27, 57–75. https://doi.org/10.1175/JCLI-D-12-00837.1.
IEA, 2020. Climate Impacts on African Hydropower. IEA, Paris (accessed 1.10.21). https://www.iea.org/reports/climate-impacts-on-african-hydropower.
Kopytkovskiy, M., Geza, M., McCray, J.E., 2015. Climate-change impacts on water resources and hydropower potential in the Upper Colorado River Basin. J. Hydrol. Reg. Stud. 3, 473–493. https://doi.org/10.1016/j.ejrh.2015.02.014.
Kummu, M., Varis, O., 2007. Sediment-related impacts due to upstream reservoir trapping, the Lower Mekong River. Geomorphology 85, 275–293. https://doi.org/10.1016/j.geomorph.2006.03.024.
Lehner, B., Czisch, G., Vassolo, S., 2005. The impact of global change on the hydropower potential of Europe: a model-based analysis. Energy Policy 33, 839–855. https://doi.org/10.1016/j.enpol.2003.10.018.
Lehner, B., Verdin, K., Jarvis, A., 2006. HydroSHEDS Technical Documentation Version 1.0. World Wildlife Fund US, Washington, DC, pp. 1–27.
Meema, T., Tachikawa, Y., 2020. Structural improvement of a kinematic wave-based distributed hydrologic model to estimate long-term river discharge in a tropical climate basin. Hydrol. Res. Lett. 14, 104–110. https://doi.org/10.3178/hrl.14.104.
Meema, T., Tachikawa, Y., Ichikawa, Y., Yorozu, K., 2020. Integrated reservoir-hydropower-hydrologic model for water resources and energy assessment. J. Japan Soc. Civ. Eng. Ser. B1 (Hydraulic Eng.). 76, I_811-I_816.
Mizuta, R., Murata, A., Ishii, M., Shiogama, H., Hibino, K., Mori, N., Arakawa, O., Imada, Y., Yoshida, K., Aoyagi, T., Kawase, H., Mori, M., Okada, Y., Shimura, T., Nagatomo, T., Ikeda, M., Endo, H., Nosaka, M., Arai, M., Takahashi, C., Tanaka, K., Takemi, T., Tachikawa, Y., Temur, K., Kamae, Y., Watanabe, M., Sasaki, H., Kitoh, A., Takayabu, I., Nakakita, E., Kimoto, M., 2017. Over 5,000 years of ensemble future climate simulations by 60-km global and 20-km regional atmospheric models. Bull. Am. Meteorol. Soc. 98, 1383–1398. https://doi.org/10.1175/BAMS-D-16-0099.1.
Mohammed, I.N., Bomblies, A., Wemple, B.C., 2015. The use of CMIP5 data to simulate climate change impacts on flow regime within the Lake Champlain Basin. J. Hydrol. Reg. Stud. 3, 160–186. https://doi.org/10.1016/j.ejrh.2015.01.002.
Mohor, G.S., Rodriguez, D.A., Tomasella, J., Siqueira Júnior, J.L., 2015. Exploratory analyses for the assessment of climate change impacts on the energy production in an Amazon run-of-river hydropower plant. J. Hydrol. Reg. Stud. 4, 41–59. https://doi.org/10.1016/j.ejrh.2015.04.003.
MRC, 2005. Hydrology of the Mekong Basin. Mekong River Commission, Vientiane.
MRC, 2018. Basin-Wide Assessment of Climate Change Impacts on Hydropower Production Final Report, 41 pp.
Nohara, D., Nishioka, Y., Hori, T., Sato, Y., 2016. Real-time Reservoir operation for flood management considering ensemble streamflow prediction and its uncertainty. Advances in Hydroinformatics, pp. 333–347. https://doi.org/10.1007/978-981-287-615-7_23.
Piman, T., Cochrane, T.A., Arias, M.E., Dat, N.D., Vonnarart, O., 2015. Managing hydropower under climate change in the Mekong tributaries. In: Shrestha, S., Anal, A.K., Salam, P.A., van der Valk, M. (Eds.), Managing Water Resources Under Climate Uncertainty. Springer International Publishing, Cham, pp. 223–248. https://doi.org/10.1007/978-3-319-10467-6_11.
Piman, T., Cochrane, T.A., Arias, M.E., 2016. Effect of proposed large dams on water flows and hydropower production in the Sekong, Sesan and Srepok rivers of the Mekong Basin. River Res. Appl. 32, 2095–2108. https://doi.org/10.1002/rra.3045.
Shrestha, S., Bajracharya, A.R., Babel, M.S., 2016. Assessment of risks due to climate change for the Upper Tamakoshi Hydropower Project in Nepal. Clim. Risk Manag. 14, 27–41. https://doi.org/10.1016/j.crm.2016.08.002.
Tanaka, T., Tachikawa, Y., 2015. Testing the applicability of a kinematic wave-based distributed hydrological model in two climatically contrasting catchments. Hydrol. Sci. J. 60, 1361–1373. https://doi.org/10.1080/02626667.2014.967693.
Tanaka, T., Kiyohara, K., Tachikawa, Y., 2020. Comparison of fluvial and pluvial flood risk curves in urban cities derived from a large ensemble climate simulation dataset: a case study in Nagoya, Japan. J. Hydrol. 584, 124706 https://doi.org/10.1016/j.jhydrol.2020.124706.
Tebaldi, C., Knutti, R., 2007. The use of the multi-model ensemble in probabilistic climate projections. Philos. Trans. R. Soc. A Math. Phys. Eng. Sci. 365, 2053–2075. https://doi.org/10.1098/rsta.2007.2076.
Thompson, J.R., Crawley, A., Kingston, D.G., 2017. Future river flows and flood extent in the Upper Niger and Inner Niger Delta: GCM-related uncertainty using the CMIP5 ensemble. Hydrol. Sci. J. 62, 2239–2265. https://doi.org/10.1080/02626667.2017.1383608.
Thornthwaite, C.W., 1948. An approach toward a rational classification of climate. Geogr. Rev. 38, 55. https://doi.org/10.2307/210739.
Trzaska, S., Schnarr, E., 2014. A Review of Downscaling Methods for Climate Change Projections. United States Agency Int. Dev. by Tetra Tech ARD, pp. 1–42.
van Vliet, M.T.H., Wiberg, D., Leduc, S., Riahi, K., 2016. Power-generation system vulnerability and adaptation to changes in climate and water resources. Nat. Clim. Chang. 6, 375–380. https://doi.org/10.1038/nclimate2903.